Università degli Studi di Padova
Dipartimento di Scienze del Farmaco

Scuola di Dottorato in Scienze Farmacologiche
Indirizzo Farmacologia Molecolare e Cellulare
XXIV Ciclo

Molecular and functional studies of REEP1
(Receptor Enhancing Expression Protein)
protein involved in Hereditary Spastic Paraplegias

Direttore della Scuola: Prof. Pietro Giusti

Coordinatore d'indirizzo: Prof. Pietro Giusti

Supervisore: Dott.ssa Paola Finotti

Supervisori esterni: Dott.ssa Genny Orso

Dott. Andrea Martinuzzi

Dottoranda : Vera De Nardo

1. INDEX

2.

ABBREVIATIONS

ER: Endoplasmic Reticulum

REEP: Receptor Expression Enhancing Protein

PDI: Protein Disulfide Isomerase

Arg: Arginine

Lys: Lysine

P: Proline

K: Lysine

A: Alanine

E: Glutammic acid

ALLN: *N*-acetyl-l-leucinyl-l-leucinyl-l-norleucinal)

MA: Methyladenine

HSP: Hereditary Spastic Paraplegia

CNS: Central Nervous System

TM: Trans-membrane domain

ORs: Odorant Receptors

GPCR: Receptor associated with G proteins

TAS: Bitter taste receptors

NE: Nuclear Envelope

NEM: N.ethylmaleimide

NSF: NEM-sensitive fusion protein

DGAT: acyl-CoA:diacylglycerol acyltransferase

ATGL: adipose tissue triacylglycerol lipase

CTP: phosphocholine cytidylyltransferase

CTT: cytidylyltransferase

V: Valine

ICC: Immunocytochemistry

PBS: Phosphate Buffered Saline

ALDI: associated with lipid droplet protein

3. ABSTRACT

Mutations in the gene encoding REEP1 protein are responsible for *SPG31*, a common autosomal dominant Hereditary Spastic Paraplegia. The biological role of REEP1 and the pathogenetic mechanism underlying disease are unknown. This project aimed to explore the function of REEP1 and the mutant variants involved in HSP pathology using different experimental approaches in mammalian cell cultures.

The studies carried out in our laboratory shown that REEP1 is involved in lipid droplets (LDs) biogenesis and its localization depends by the cell energetic balance; also it has the characteristic of forming oligomers to makes its function. We first demonstrated that REEP1 is localizes to ER membranes, with both the extremities C- and N- terminal face the cytoplasm; its trasmembrane domain appear too short to be inserted into the phospholipidic bilayer of ER membrane; but it is possible that the first transmembrane domain is inserted only in the external ER phospholipidic layer. This is supported by the evidence that REEP1 localization changes, going from ER to the LDs monolayer when the lipid metabolism was increased or the protein synthesis inhibited, . The relocation of REEP1 in LDs is supported by the theory that ER membranes are the site of LDs biogenesis: LDs grow between the ER phospholipidic bilayer and after they or break away or extrude from ER remain anchored to ER by a stalk. This hypothesis is supported by the presence of ER resident protein in LDs membranes: these proteins can shift from ER to LDs after a intra cellular signal, and *vice versa*.

We then focused our attention to REEP1 pathological mutations. REEP1^{P19R}, a missense mutation with an aminoacidic substitution in the first transmembrane domain. We demonstrated that REEP1^{P19R} localizes on LDs membranes and relocates to the ER when fatty acids synthesis is inhibited. Moreover we shown that this pathological mutation prevents REEP1 oligomerization. REEP1^{A132V} is a missense mutation that present the aminoacidic substitution in a site supposed to be important for microtubules binding. Indeed REEP1^{A132V} localizes to ER membranes and partially overlaps the microtubules cythoskelethon. These results suggest a REEP1 function in LDs metabolism and open new perspectives to understand the of HSPs pathogenic mechanism and the process of neurodegeneration.

4. ABSTRACT

Mutazioni nella proteina REEP1, codificata dal gene *SPG31*, sono responsabili di una comune forma autosomica dominante di Paraplegia Spastica Ereditaria (HSP).

La funzione biologica di REEP1 e i meccanismi patogenetici che si trovano dietro a questa malattia rimangono ad oggi sconosciuti.

Questo progetto ha lo scopo di investigare la funzione di REEP1 e delle sue mutazioni attraverso differenti approci sperimentali che prevedono l'uso di colture cellulari di mammifero.

Studi svolti nel nostro laboratorio hanno dimostrato che REEP1 è coinvolto nella biogenesi dei *lipid droplets* (LDs) e che la sua localizzazione dipende dal bilancio energetico della cellula; inoltre questa proteina ha anche la caratteristica di formare oligomeri per poter svolgere la propria funzione.

Inizialmente abbiamo dimostrato che REEP1 è localizzato sulla membrana del reticolo endoplasmatico (ER), con entrambe le sue estremità N- e C- terminali rivolte verso il citoplasma della cellula, mentre il dominio trans membrana della proteina sembra troppo corto per poter attraversare interamente il doppio strato fosfolipidico della membrana del ER; è però possibile che REEP1 sia inserita solo nello strato fosfolipidico esterno. Questa ipotesi è avvalorata dal fatto che quando il metabolismo lipidico viene incrementato o la sintesi proteica inibita, la localizzazione di REEP1 cambia, spostandosi dal reticolo ai LDs; inoltre il reticolo endoplasmatico è anche la sede di biogenesi dei LDs, in particolare sembra che i LDs crescano all'interno del doppio strato fosfolipidico del reticolo endoplasmatico per poi essere definitivamente separati dal reticolo oppure, e questa sembra l'ipotesi più probabile, estrusi dal reticolo, rimanendo però attaccati ad esso tramite una lunga lamella di membrana fosfolipidica detta "stelo". Ci sono infatti delle proteine di membrana che si trovano sia sul reticolo che sulla membrana dei LDs: queste proteine possono quindi spostarsi lungo la membrana passando dal reticolo ai LDs dopo l'attivazione di opportuni segnali intracellulari, e viceversa.

Successivamente ci siamo focalizzati sulle mutazioni patologiche di REEP1: REEP1^{P19R} è una mutazione missenso che presenta una sostituzione amminoacidica nel primo dominio transmembrana. Abbiamo dimostrato che REEP1^{P19R} è localizzata sulla

membrane dei LDs e viene spostata sulla membrana del reticolo endoplasmatico quando la sintesi degli acidi grassi viene inibita. Inoltre abbiamo evidenziato che questa mutazione patologica non è in grado di dimerizzare.

REEP1^{A132V} è una mutazione missenso che presenta una sostituzione amminoacidica in una posizione che si suppone essere importante in quanto sito di legame con i microtubuli. Inoltre REEP1^{A132V} è localizzata sulla membrane del ER ma è anche parzialmente sovrapposta ai microtubuli. Questi risultati suggeriscono che REEP1 possa avere una funzione nel metabolismo dei LDs e aprono nuove prospettive per quanto riguarda il meccanismo patologico e i processi neurodegenerativi causati da HSP.

5. INTRODUCTION

1. HEREDITARY SPASTIC PARAPLEGIA

Hereditary spastic paraplegia (HSP) was first described by Strümpell in 1880 as a neurodegenerative disorder.

At present, HSP is used to describe a group of genetically and clinically heterogeneous neurodegenerative disorders in which the predominant feature is the progressive spasticity associated with mild weakness of the lower extremities, which may be accompanied by urinary urgency and subtle vibratory sense impairment (McDermott, White et al. 2000).

Neuropathological analysis of tissues from patients with HSP has revealed axonal degeneration of the distal portions of the corticospinal tracts and the spinocerebellar tracts, which together constitute the longest motor and sensory axons of the central nervous system (CNS) (Figure) (Schwarz and Liu 1956; Behan and Maia 1974; Reid 1997).
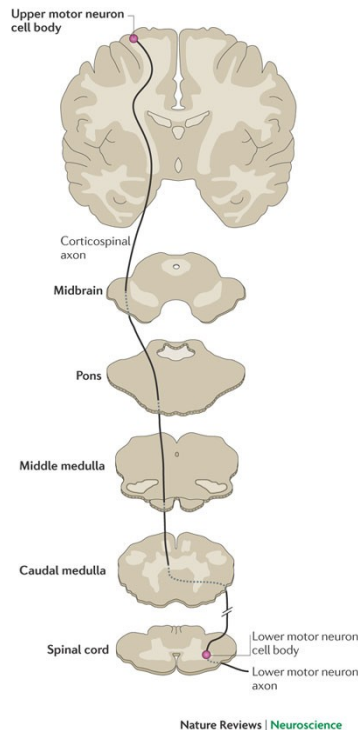

Figure : The corticospinal tract

Clinically these disorders are conventionally subdivided into "pure" (or "uncomplicated") forms, when the above features occur in isolation, and "complicated"

forms in the presence of additional neurologic or systemic impairments such as mental retardation, cerebellar ataxia, dementia, optic atrophy, retinopathy, extrapyramidal disturbance, epilepsy and motor neuropathy (Harding 1993; Reid 1997). Age of symptom onset, rate of progression, and degree of disability are often variable between different genetic types of HSP, as well as within individual families in which all subjects have precisely the same HSP gene mutation.

HSPs may have autosomal dominant, recessive and X-linked inheritance (Table ,Table ,Table). To date loci have been mapped on different chromosomes. Fifteen loci segregate with autosomal dominant (AD) forms, twenty follow an autosomal recessive pattern of inheritance and three *loci* lie on the X chromosome (Depienne, Stevanin et al., 2007) Despite the daunting number of distinct genetic loci, well over 50% of HSP patients harbor pathogenic mutations in 1 of just 3 genes: spastin (SPG4, also known as SPAST), atlastin-1 (SPG3A), also known as ATL1, or receptor expression enhancing protein1 (REEP1, also known as SPG31) (Seong et al., 2010).

Locus	Chromosome region	Gene or protein	Discriminating features	Reference
Pure forms				
SPG3A	14q12–q21	Atlastin	Predominantly early onset	MIM182600 [2,3[•],4[••],5]
SPG4	2p22	Spastin		MIM182601 [4[••],5–8,9[•],10[•], 11,12[•],13–16,17[••]]
SPG6	15q11.2–q12	NIPA1	Predominantly adult onset	MIM600363
SPG8	8q24	KIAA0196	Predominantly adult onset	MIM603563 [18[•]]
SPG10	12q13	KIF5A	Predominantly early onset	MIM604187 [19]
SPG12	19q13	Unknown	Predominantly early onset	MIM604805
SPG13	2q24–q34	HSP60	Predominantly adult onset	MIM605280
SPG19	9q33–q34	Unknown	Predominantly adult onset	MIM607152
SPG31	2p12	REEP1		MIM610250 [20[•]]
SPG33	10q24.2	ZFYVE27		MIM610244 [21[•]]
SPG37	8p21.1–q13.3	Unknown		[22[•]]
Complex forms				
SAX1	12p13	Unknown	Spastic ataxia	MIM108600 [23]
SPG9	10q23.3–q24.2	Unknown	Cataract, motor neuropathy, short stature, skeletal abnormalities, gastro-oesophageal reflux	MIM601162
SPG17	11q12–q14	BSCL2/Seipin	Silver syndrome – severe distal wasting	MIM270685 [24]
SPG29	1p31–p21	Unknown	Sensorineural hearing impairment, pes cavus, neonatal hyperbilirubinemia without kernicterus, hiatal hernia	MIM609727

MIM, Mendelian Inheritance in Man at http://www.ncbi.nlm.nih.gov/sites/entrez?db=OMIM.

Table : Autosomal dominant forms of hereditary spastic paraplegias (Depienne, Stevanin et al., 2007)

Gene	Protein	Locus	Age at onset (years)	Associated signs	Number of families	Reference
SPG1	L1CAM	Xq28	Infancy	Corpus callosum hypoplasia, retardation, adducted thumbs, spastic paraplegia, hydrocephalus	>100 but few with the spastic paraplegia phenotype	MIM303350
SPG2	PLP	Xq21	1–18	Quadriparesis, congenital nystagmus, mental retardation, seizures	>75 but few with the spastic paraplegia phenotype	MIM312920
SPG16	Unknown	Xq11.2	Infancy	Pure (severe)	1	MIM300206

Table : Autosomal dominant forms of hereditary spastic paraplegias (Depienne, Stevanin et al.,

Gene	Protein	Locus	Age at onset (years)	Associated signs	Origin and number of families	Reference
Pure forms						
SPG5	Unknown	8p	1–40		>12 families	MIM270800 [31]
SPG24	Unknown	13q	1		Saudi-Arabia ($n=1$)	MIM607584 [28]
SPG28	Unknown	14q	6–15		Morocco ($n=1$)	MIM609340 [29]
SPG30	Unknown	2q	12–21		Algeria ($n=1$)	MIM610357 [30]
Complex forms						
SPG7	Paraplegin	16q	11–42	Cerebellar signs, PNP, pes cavus, optic atrophy	Many	MIM602783 [26,27,32–34]
SPG14	Unknown	3q	~30	Distal motor neuropathy, mental retardation, pes cavus, visual agnosia	Italy ($n=1$)	MIM605229
SPG27	Unknown	10q	2–45	Cerebellar ataxia, PNP, mental retardation, microcephaly, facial and skeletal dysmorphia, blepharophimosis	French Canadian and Tunisia ($n=2$)	MIM609041
SPG11 (AR-HSP-TCC)	Spatacsin	15q	1–23	Mental retardation or cognitive impairment, PNP, TCC	Mediterranean basin, Japan ($n>30$)	MIM610844 [35–37,38••]
SPG15 (Kjellin syndrome)	Unknown	14q	13–23	Pigmented maculopathy, wasting, dysarthria, cerebellar signs, mental retardation	Ireland, Arabian families ($n=5$)	MIM270700 [39]
SPG20 (Troyer syndrome)	Spartin	13q	Early childhood	Mental retardation, cerebellar signs, developmental delay and short stature	Amish founder	MIM275900
SPG21 (Mast syndrome)	Maspardin	15q	20–40	Extrapyramidal syndrome, premature aging, cognitive decline, dysarthria, TCC, periventricular white matter hyperintensities, cataract, dystonia, cerebellar signs, PNP, chorea, distal wasting	Amish founder	MIM248900
SPG23 (Lison syndrome)	Unknown	1q	Early childhood	Abnormalities of skin and hair pigmentation, facial and skeletal dysmorphia, postural tremor, cognitive impairment, premature aging	Arab-Israelian ($n=1$)	MIM270750
SPG25	Unknown	6q	30–46	Prolapsed intervertebral disks, multiple disc herniation, bilateral cataract, congenital glaucoma	Italy ($n=1$)	MIM608220
SPG26	Unknown	12cen	22–42	Intellectual impairment, distal muscle wasting, dysarthria, PNP	Kuwait and Spain ($n=2$)	MIM609105
SPG32	Unknown	14q	6–7	Pontine dysraphia, mental retardation, TCC	Portugal ($n=1$)	MIM611251 [40]
TCC + epilepsy	Unknown	8q	1–7	Mental deterioration, epilepsy, TCC	Saudi-Arabia ($n=2$)	[41]
SPOAN	Unknown	11q	Infancy	Optic atrophy, PNP	Brazil ($n=1$)	MIM609541
ARSACS	Sacsin	13q	Early childhood	Ataxia, dysarthria, distal wasting, nystagmus, retinal striation, PNP	Quebec, Japan, Mediterranean basin	MIM270550 [42–47]
ARSAL	Unknown	2q	Variable	Spastic ataxia with leucodystrophy	Quebec ($n=17$)	[48]
SAX2	Unknown	17p	Variable	Cerebellar ataxia, dysarthria	Morocco, Algeria, France ($n=4$)	[49]

MIM, Mendelian Inheritance in Man at http://www.ncbi.nlm.nih.gov/sites/entrez?db=OMIM; PNP, polyneuropathy; AR, autosomal recessive; TCC, thin corpus callosum; SPOAN, spastic paraplegia, optic atrophy, and neuropathy; ARSACS, autosomal recessive spastic ataxia of Charlevoix Saguenay; ARSAL, autosomal recessive spastic ataxia with frequent leucoencephalopathy; SAX2, spastic ataxia 2.

Table : X-linked forms of hereditary spastic paraplegias (Depienne, Stevanin et al., 2007)

Differential diagnosis is now becoming easier because of the availability of more precise and sophisticated neuroradiological investigation techniques, biochemical tests and genetic analysis. The very recent discovery of many HSP genes is rapidly shaping new concepts of the pathophysiologic mechanisms of HSP. Whereas the uniform clinical appearance of uncomplicated HSPs initially suggested that a common biochemical disturbance underlies most types of HSP, this appears to not be the case. Rather, it appears that very long central nervous system axons (i.e., corticospinal tracts

and dorsal column fibers are particularly vulnerable to a number of distinct biochemical disturbances and that the highly similar clinical features of genetically diverse types of uncomplicated HSP reflect the limited repertoire of symptoms from corticospinal tracts and, to a lesser extent, dorsal column fiber disturbance.

Recently, there have been substantial advances in understanding of the function of this large group of HSP-associated proteins involved with membrane trafficking (Figure) (Blackstone, 2011).
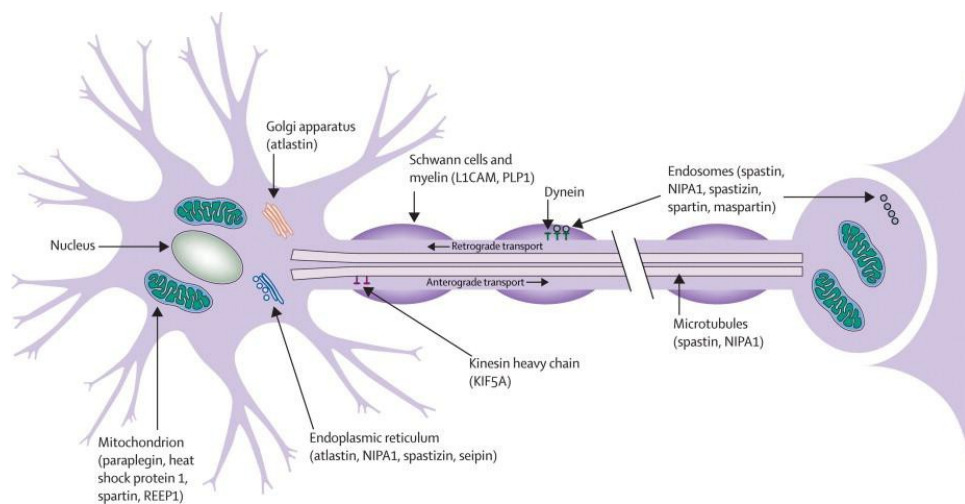

Figure : Neuron schematic representation of the possible pathological mechanisms of the mutated proteins involved in HSP. (Blackstone, 2011)

At this stage, five different molecular processes appear to be involved in different genetic types of HSP.

1) Myelin composition affecting long, central nervous system axons. X-linked SPG2 HSP is due to proteolipid protein gene mutation, an intrinsic myelin protein (Dube, Mlodzienski et al., 1997).

2) Embryonic development of corticospinal tracts. X-linked SPG1 is due to mutations in L1 cell adhesion molecule which plays a critical role in the embryonic differentiation of corticospinal tracts guidance of neurite outgrowth during

development, neuronal cell migration, and neuronal cell survival (Kenwrick, Watkins et al., 2000).

3) Oxidative phosphorylation deficit. Two HSP genes (SPG7/paraplegin and SPG13/chaperonin 60) encode mitochondrial proteins (Hansen, Durr et al., 2002). Abnormal appearing mitochondria (ragged red fibers) and cytochrome C oxidase deficient fibers are noted in muscle biopsies of some (but not all) subjects with SPG7/parapegin mutation.(articolo su REEP1, difetti mitocondriali)

4) Axonal transport. SPG10 autosomal dominant HSP is due to mutations in kinesin heavy chain (KIF5A) a molecular motor that participates in the intracellular movement of organelles and macromolecules along microtubules in both anterograde and retrograde directions (Reid, Kloos et al., 2002).All KIF5A mutations are missense mutations and tipically impair transport as they affect the kinesin motor domain.(Reid, et al., 2002, Goizet, et al., 2009, Schule, et al., 2008). The efficiency of cargo transport to the distal axon is thought to be affected motors for cargo her because the mutated KIF5A are slower motors or because they have reduced microtubule binding affinity and compete with other, wild-type motors for cargo binding sites (Ebbing, et al., 2008).

5) Cytoskeletal disturbance. Spastin (SPG4) is a microtubule severing protein whose mutations are pathogenic through a disturbance in the axonal cytoskeleton (Errico, Ballabio, et al., 2002).

There is currently no "cure" for HSP. Physical therapy accompanying with a regular exercise and stretching program play an important role in treating HSP symptoms (Fink, 2003). While exercise or physical therapy do not prevent or reverse the damage to the nerve fibers, it will help HSP patients in maintaining mobility, retaining or improving muscle strenght, minimizing atrophy of the muscles due to disuse, increasing endurance (and reducing fatigue), preventing spasms and cramps, maintaining or improving range of motion, and providing cardiovascular conditioning.

2. RECEPTOR EXPRESSION ENHANCING PROTEIN (REEP1)

2.1. The SPG31 gene

All of the SPG31 mutations lead to a pure form of HSP (on chromosome 2p12 (Züchner, et al., 2006) with a variable age of onset. Most people HSP affected have the outbreak of the pathology in the first and in the second decades of their life; whereas only the 15% of the people present an age of onset after 30 years. It is relatively common, and mutations in the REEP1 gene have been identified in 3% of a sample of unrelated patients with HSP, which increased to 8-2% in pure HSP if those with SPG3A and SPG4 (SPAST) mutations were excluded. (Beetz et al., 2008). Beyond the missense mutations, the most common SPG31 alterations are little insertions o deletions that cause a reading frameshift, and produce premature stop codons. Another mutations class in this gene is the distribution of the splicing canonic sites that generate frameshift mutations. Finally, it's possible to find mutations in 3'-URT sequence that altered the RNAi site recognition (Zuchner et al, 2006). The SPG31 gene consist of 7 exons.

2.2. Human REEP1

The *SPG31* gene encodes a 201 amino-acid protein REEP1 (Figure). REEP1 is a member of the REEP/DP1/Yop1p superfamily; *in silico* analyses of REEP1 predicted two transmembrane domains (TM1 e TM2) and the conserved protein domain, called "deleted in polyposis", TB2/DP1/HVA22, with unknown function.
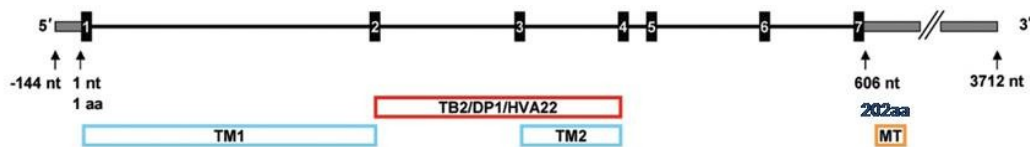

Figure : Schematic representation of *SPG31* gene (Züchner *et al.*, 2006).

This family contains some types of eucariotic proteins. It's included:
- The TB2/DP1 (deleted in polyposis) protein, its loss cause seriously form of familial adenoma- polyposis, an hereditary autosomal dominant oncological

pathology.

- The HVA22 barley protein that was activated in stressed cells by absissic acid; it has a regulatory function in the membrane turnover or in decrease the level of the unnecessary secretions.

- The yeast *Saccharomyces cervisiae* protein, Yop1p that was involved in the tubules formation of the endoplasmic reticulum.

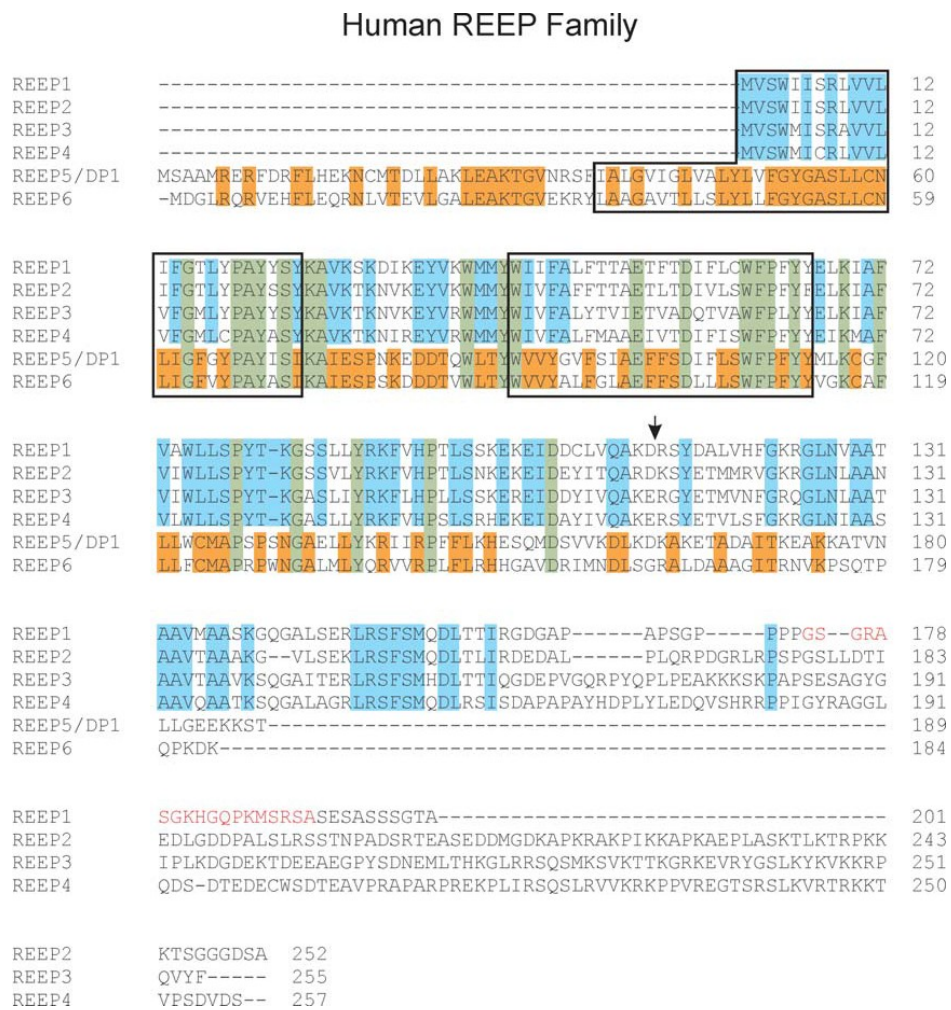- Moreover, in human there are six REEP proteins (REEP1-6) (Figure)

Figure : Schematic representation of human REEP proteins (Züchner *et al.*, 2006.).

There is a phylogenetic division of REEP proteins into two subfamily based on the sequences similarity (Figure).
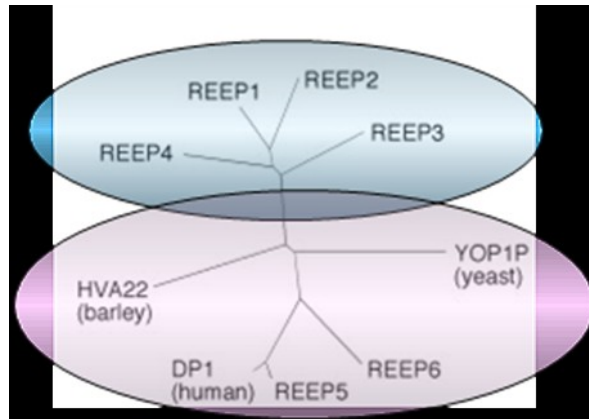
Figure : Phylogenetic division of REEP proteins family members (Saito *et al.*, 2004).

In the first subfamily we can find REEP1-4, meanwhile, in the second, REEP5-6. The first group presents a smaller initial hydrophobic segment, and the absence of a N-terminal cytoplasmatic domain with a C-terminal part most longer than REEP5-6.

REEP sequence is more similar in other species: *Drosophyla melanogaster*, *Stronglyocentrotus purpuratus* and *Caenorhabditis elegans*. The yeast protein Yop1, the only protein of the TB2_DP1_HVA22 superfamily, is structurally similar to REEP5-6 and its suggest that the REEP1-4 proteins have a different function from human proteins REEP5-6 and yeast protein Yop1, that are involved in ER remodeling (Voeltz et al., 2006).

2.3. Hypothesis on REEP1 function

2.3.1. REEP1 may be involved in folding, transport and recognizing of odorant receptor

Two different groups supposed that REEP1 may be involved in the expression of some types of chemo-receptors, like the odorant receptors (ORs) and the bitter taste receptors (TAS2R) on the cellular membrane (Saito et al., 2004; Behrens, et al., 2006).

These sensorial receptors are associated with G proteins (GPCR), GPCR required accessory proteins for their right expression on cellular membrane (Brady et al., 2002). These receptors are synthesized in the ER and transported to cilia and dendrites (Barnea et al., 2004). The GPCR expression is a difficult process that comprehend the protein assembly, the post-trasductional modifications and the transportation through the cellular compartements. (Figure).

REEP1, with *RTP1* and *RTP2* genes, may be involved in whatever phase of this development (Saito et al., 2004)

Moreover, REEP1 may be caused the correct assembly of these receptors. The homologue gene of *REEP1* in plants *HVA22*, it's a gene that is expressed under stress conditions and it is possible that HVA22 may be to act as a chaperonin (Chen et al., 2002). The homologue gene of *REEP1* in yeast, Yop1p is involved in proteins transport from ER to Golgi. This suggest that REEP1 to make easier the vesicles transport with receptors inside (Hicke et al., 1989). Finally REEP1 may behaved like co-receptor that hide an ER retention signal for.
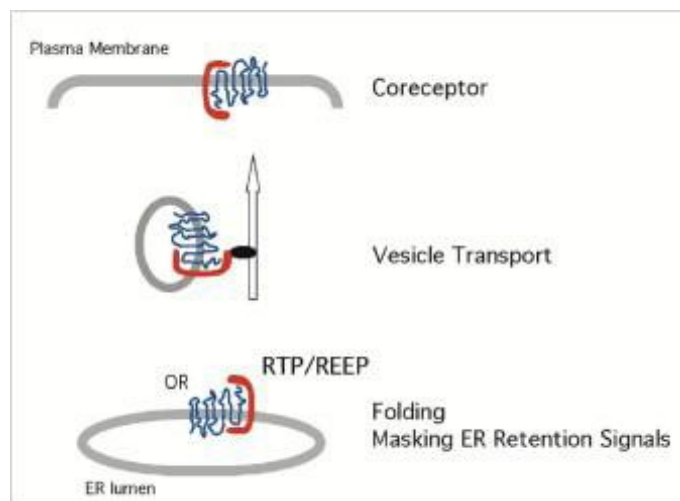

Figure : Schematic representation of the possible REEP1 function in odorant receptor expression(Saito *et al.*, 2004).

2.3.2. REEP1, spastin and atlastin-1 coordinate microtubule interaction with the tubular ER network

REEP1 is a member of the DP1/Yop1p family of ER-shaping proteins that can interacts with both atlastin-1 and an isoform of the microtubule severing ATPase spastin localizes to the ER and contains a hairpin loop domain, giving rise to a protein complex with pathogenic significance for a majority of HSP cases. Unexpectedly, REEP1 also mediates interaction of ER tubules with the microtubule cytoskeleton through its C-terminal cytoplasmic domain, and in fact defines a novel family within the larger DP1/Yop1p superfamily. In this regard, the ER phenotype upon REEP1 overexpression, characterized by ER tubules closely aligned with thickened, bundled microtubules, is

similar to that observed for the *SPG4* missense mutant spastin p.K388R that lacks ATPase activity and microtubule-severing activity but retains the ability to bind microtubules (Connell et al., 2009; Yabe et al., 2002). Furthermore, both REEP1 and spastin interact with Atlastin-1 as well as ER-shaping proteins, such as the reticulons (Figure) (Evans et al., 2006; Sanderson et al., 2006; Mannan et al., 2006).

REEP1, like spastin, interacts with the microtubule cytoskeleton and this suggests an important role for the microtubule cytoskeleton in the distribution of the ER network, which is particularly relevant for the long axonal processes of highly polarized corticospinal motor neurons that can extend up to 1 meter in length in humans (Soderblom et al., 2006).

Interestingly, though REEP1 and the closely related protein REEP2 interact with microtubules and redistribute ER tubules along the microtubule cytoskeleton, DP1/REEP5 and REEP6 do not (Shibata et al., 2008; Zuchner et al., 2006). It will be important to determine in future studies whether microtubule interactions are a general feature of all members of REEP1–4 that distinguishes them from REEP5-6.

Indeed, such an adaptation may reflect the increased importance of ER-microtubule interactions in forming and distributing the ER network in higher species, particularly within highly polarized cells, such as the corticospinal neurons that are selectively affected in the HSPs. Along these lines, the budding yeast *S. cerevisiae* has only 1 DP1/Yop1p superfamily member, Yop1p, which is structurally and functionally related to REEP5–6 proteins. Since *S. cerevisiae* generates ER tubules along actin filaments, there may be no need for a REEP1–4 ortholog.
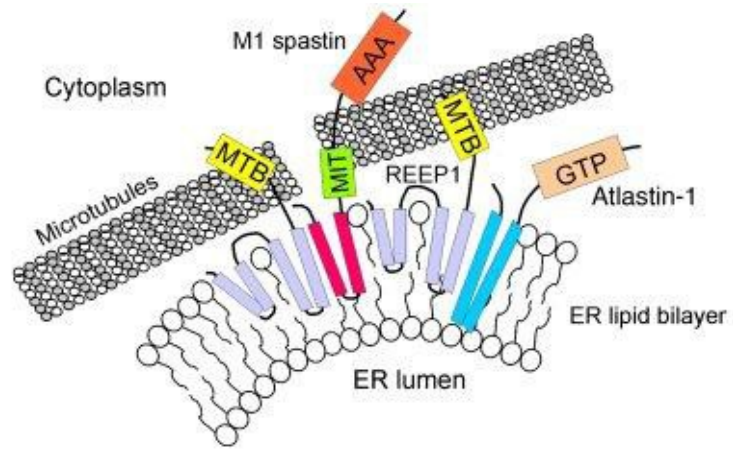
Figure : Interation model between the proteins involved in HSP in the modulation of ER morphology. (Park *et al.*, 2010).

3. THE ENDOPLASMIC RETICULUM (ER)

3.1. ER structure and organization

The endoplasmic reticulum (ER) is a single compartment: it has a single membrane system with a continuous intralumenal space (Dayel and Verkman, 1999).

ER has many different functions. These include the translocation of proteins (such as secretory proteins) across the ER membrane, the integration of proteins into the membrane, the folding and modification of proteins in the ER lumen, the synthesis of phospholipids and steroids on the cytosolic side of the ER membrane, the storage of calcium ions in the ER lumen and their regulated release into the cytosol. The interphase ER can be divided into nuclear and peripheral ER. The nuclear ER, or nuclear envelope (NE), consists of two sheets of membranes with a lumen. The NE surrounds the nucleus, with the inner and outer membranes connecting only at the nuclear pores, and is underlaid by a network of lamins. The peripheral ER is a network of interconnected tubules that extends throughout the cell cytoplasm. The lumenal space of the peripheral ER is continuous with that of the nuclear envelope and together they can comprise >10% of the total cell volume (Terasaki and Jaffe, 1991).

3.2. ER dynamics

In interphase cells, the peripheral ER is a dynamic network consisting of cisternal sheets, linear tubules, polygonal reticulum and three-way junctions (Allan and Vale, 1991). Several basic movements contribute to its dynamics: elongation and retraction of tubules, tubule branching, sliding of tubule junctions and the disappearance of polygons. These movements are constantly rearranging the ER network while maintaining its characteristic structure.

The dynamics of the ER network depend on the cytoskeleton. In mammalian tissue culture cells, goldfish scale cells, and *Xenopus* and sea urchin embryos the ER tubules often co-align with microtubules. Microtubule-based ER dynamics were studied with time-lapse microscopy and appear to be based on three different mechanisms. First, new ER tubules can be pulled out of existing tubules by motor proteins migrating along microtubules. Secondly, new tubules may be dragged along by the tips of polymerizing microtubules. Finally, ER tubules may associate with the sides of microtubules, via motor proteins, as they slide along other microtubules. Each of these mechanisms can

lead to tubule extension and, when tubules intersect, they fuse and create three-way junctions (Allan and Vale, 1991; Waterman-Storer and Salmon, 1998).

The cytoskeleton contributes to ER dynamics, but it is not necessary for the maintenance of the existing ER network. Although depolymerization of microtubules by nocodazole in mammalian tissue culture cells inhibits new tubule growth and causes some retraction of ER tubules from the cell periphery, the basic tubular-cisternal structure of the ER remains intact (Terasaki et al., 1986).

Similarly, actin depolymerization in yeast blocks ER movements but does not disrupt its structure (Prinz et al., 2000).

3.3. Formation and maintenance of ER network

Little is known about how the particular architecture of the ER is formed and maintained. It is known that the cytoskeleton is not necessary for the formation of a tubular network *in vitro*. In *Xenopus* egg extracts, ER networks can form *de novo* and this process is not affected by the addition of inhibitors of microtubule polymerization, by the depletion of tubulin from the extract or by inhibitors of actin polymerization (Dreier and Rapoport, 2000).

In contrast, homotypic membrane fusion is essential for preserving the typical structure of the ER (Vedrenne and Hauri, 2006), and its failure prevents the formation of an intact ER network (Dreier and Rapoport, 2000). Homotypic fusion of ER membranes depends categorically on GTP hydrolysis and does not require cytosolic proteins or ATP (Dreier and Rapoport, 2000; Voeltz et al., 2006), suggesting the involvement of a GTP-dependent fusion machinery tightly associated with the ER membrane. Inhibition of network formation by GTPγS and N-ethylmaleimide (NEM) (Allan and Vale, 1991; Dreier and Rapoport, 2000), suggests that a GTPase and/or a factor similar to the NEM-sensitive fusion protein (NSF) may be involved. There is some evidence that a homolog of NSF, p97, and its co-factor p47, contribute to efficient ER network formation in *Xenopus* egg extracts (Hetzer et al., 2001), and the yeast homolog of p97, Cdc48, has been shown to be involved in homotypic ER fusion (Latterich et al., 1995). A role for p97/p47 in the *in vitro* formation of the transitional ER has also been suggested (Roy et al., 2000). Surprisingly, however, a mutant of Cdc48 does not affect ER structure in yeast (Prinz et al., 2000). The involvement of these proteins in ER membrane fusion is

indirect and neither exhibits GTPase function. Thus, the molecular components of the GTP-dependent activity responsible for homotypic fusion of ER membranes have not yet been identified.

3.4. Tubulation of ER membranes

Membrane tubules are a structural feature of both the ER and the Golgi complex (Lee et al., 1989; Dreier and Rapoport, 2000). Both types of tubule have similar diameters (50–100 nm), whether formed *in vitro* or *in vivo*, and in the case of the ER, tubule diameter is conserved from yeast to mammalian cells, suggesting that their formation is a regulated and fundamental process.

The mechanism behind tubulation is unclear. Perhaps the most plausible models for tubule formation and maintenance are based on mechanisms that generate or stabilize high curvature in membranes.

Tubules have a unique curvature of the lipid bilayer. Proteins would be required to keep the lipid imbalance or to create curvature on their own. Two class of proteins are necessary for the generation of tubular ER: the reticulons and DP1/Yop1p. They have been proposed to be involved in stabilization of high curvature membranes by means of the hairpin formed inside the membrane by the two hydrophobic segments in these proteins (Voeltz et al., 2006).

4. LIPID DROPLETS (LDs)

Lipid droplets were for many years envisaged as simple storage organelles for lipids but are now considered multi-functional organelles with additional roles in lipid homeostasis, cell signaling, and intracellular vesicle trafficking (Wang et al., 1999; Liu et al., 2003; Umlauf et al., 2004). The essential structure of the lipid droplets is of a hydrophobic core of neutral lipids surrounded by a phospholipid monolayer. Freezefracture electron microscopy has demonstrated that the hydrophobic lipid core - once thought to be homogeneous - in fact often has an elaborate structure of lamellar stacks and/or concentrically arranged layers (Robenek et al., 2009). The ER is the site of lipid droplet formation. A widely promoted idea is that cholesterol ester and triglycerides, synthesized by ACAT and DGAT, accumulate within the lipid bilayer of the ER membrane and, upon reaching a critical size, the accumulation is pinched off into the cytoplasm as a lipid droplet enveloped in a phospholipid monolayer formed from the cytoplasmic leaflet of the ER membrane (Brown, 2001; Murphy, 2001). A variation on this idea proposes that the intramembrane lipid accumulation is released with portions both of the cytoplasmic and luminal phospholipid monolayer leaflets of the ER membrane (Ploegh, 2007). However, lipid accumulations within the ER membrane have never been observed. Freezefracture electron microscopy demonstrates that growing lipid droplets are intimately associated with but lie external to specialized cup-like sites of the ER membrane (Robenek et al., 2004, 2006).

4.1. LDs composition

LDs consist of an organic core comprising neutral lipids (mainly triacylglycerols and sterol esters) that is bounded by a monolayer of phospholipids (Bartz et al., 2007a). This structure provides a unique separation of the aqueous and organic phases of the cell. Several types of proteins decorate LDs, including structural proteins (for example the proteins of perilipin family) (Brasaemble, 2007), lipid-synthesis enzymes (acetyl coenzyme A carboxylase, acyl-CoA syntetase and acyl-CoA:diacylglycerol acyltransferase 2 (DGAT2)) (Kuerschner et al., 2008; Stone et al., 2009), lipases [e.g. adipose tissue triacylglycerol lipase (ATGL)] and membrane-trafficking proteins (e.g. Rab5, Rab18 and ARF1). Adding to the complexity, different LDs in a cell can contain different proteins (Ducharme and Bickel, 2008) and have different rates of acquiring

triacylglycerol (Kuerschner et al., 2008). This suggests that cells contain distinct types of LDs with specialized functions.

Considering the composition of LDs, it is not well understood how proteins target to LDs and how this localization is regulated. Conceptually, proteins that contain transmembrane-spanning domains with hydrophilic domains on either side of a membrane bilayer cannot target to the monolayer surface of an LD; instead, there are at least two probable alternative mechanisms. First, proteins might use long membrane-embedded domains that enter and exit the membrane on the same side of the lipid monolayer. This mechanism was postulated for caveolins, which target to specialized domains of the plasma membrane and LDs (Martin and Parton, 2006), and for the lipid-synthesis enzyme DGAT2 (Kuerschner et al., 2008; Stone et al., 2006). Second, proteins might bind LD surfaces as peripheral membrane proteins by embedding an amphipathic helix. Examples include members of the perilipin family of proteins [e.g. perilipin, adipophilin, S3-12 and tail-interacting protein of 47 kDa (TIP47)] (Brasaemle, 2007). Whether a recently identified N-terminal hydrophobic sequence shared between several LD proteins [e.g. the putative methyltransferases AAM-B (methyltransferase-like protein 7A) and ALDI (associated with lipid droplet protein 1)] uses a similar targeting mechanism remains to be determined (Zehmer et al., 2008). Surprisingly, a variety of proteins have been detected in the hydrophobic core of LDs (Robenek et al., 2005), including the perilipin family of proteins. How such proteins are transported in and out of LDs, however, and whether they are natively folded in the LD are not clear.

4.2. LDs formation

The life cycle of LDs begins when fatty acids that are carried extracellularly by albumin and lipoproteins enter cells. Fatty acids are released from triacylglycerols in lipoproteins by lipoprotein lipase, and enter cells by passive diffusion facilitated by fatty-acid transport proteins or fatty-acid translocase (Ehehalt et al., 2006; Schaffer and Lodish, 1994). Fatty acids can also be synthesized de novo from carbohydrates in many cell types.

Next, fatty acids enter a bioactive pool through conjugation to CoA, forming fatty acyl-CoA, in an energy-requiring reaction. Fatty acyl-CoA is used by glycerolipid-synthesis enzymes (glycerol-3-phosphate acyltransferase and *sn*-1-acylglycerol-3-phosphate acyltransferase) in the ER to finally generate diacylglycerols. Diacylglycerols

are either converted to neutral lipids (triacylglycerols) by DGAT enzymes or enter phospholipid-synthesis pathways. How the flux between these pathways is regulated is unknown.

In contrast to fatty acids, sterols are primarily taken up into cells through endocytosis and lysosomal degradation of lipoproteins.

Thus, neutral lipids that are found in LD cores are synthesized in the ER. How these lipids accumulate and form LDs is mostly unknown. The canonical model posits that neutral lipids form a lens of oil in the ER bilayer that subsequently `buds' from the membrane (the ER-budding model) (Figure I), taking with it phospholipids from the cytosolic leaflet. Although the model has substantial support, this process has not been observed directly. In a variant of this model, the ER-domain model, LDs remain connected to the ER and are lipid-containing protrusions of the ER membrane, forming a specialized ER domain.

Another models for LD formation have been proposed. In the bicelle model (Ploegh, 2007), neutral lipids accumulate between the leaflets of the ER membrane but, instead of budding, nascent LDs are excised from the membrane, taking with them phospholipids from both the cytosolic and luminal leaflets (Figure II). This model was suggested to explain how large unfolded proteins or viruses might escape from the ER lumen into the cytosol. In the vesicular-budding model (Walther and Farese, 2008), small bilayer vesicles that remain tethered to the ER membrane are used as a platform for making LDs. Newly synthesized neutral lipids are pumped into the vesicle bilayer and fill the intermembrane space, eventually squeezing the vesicular lumen so that it becomes a small inclusion inside the LDs (Figure III). Clues that help to decipher how LDs are formed might be provided by studying seipin, an ER protein that is integral to LD formation (Fei et al., 2008; Szymanski et al., 2007).

In lipoprotein-producing cells, such as intestinal enterocytes or hepatocytes, neutral lipids can also be directed from the ER bilayer into the ER lumen to associate with apolipoprotein B for secretion (Fujimoto et al., 2008). How the amount of neutral lipids entering the storage versus the secretion pathway is determined is mostly unknown.

Figure : LDs biogenesis models (*Journal of Cell Bioscience, 2009*)

4.3. LDs growth

The size of LDs varies tremendously, with diameters ranging from as small as 20-40 nm (Stobart et al., 1986) to 100 μm (in white adipocytes), and, clearly, LDs can grow in size.

One possibility is that LDs, like balloons, expand as single organelles. If LDs remain attached to the ER, proteins and newly synthesized lipids could diffuse laterally to the LDs. If LDs are detached from the ER, these proteins and lipids must be transported to the LDs, perhaps via vesicular transport. This would pose a problem of topology, as a vesicular bilayer membrane would have to fuse with a monolayer surface at the LD. Alternatively, neutral lipids in the core could be produced locally by enzymes, such as DGATs, that are targeted to the LD surface. In either way, the increase in volume of neutral lipids would need to be matched by a corresponding increase of phospholipids at the surface. In agreement with this notion, a key enzyme of phospholipid synthesis, CTP:phosphocholine cytidylyltransferase (CCT), is localized to LD surfaces during their growth (Guo et al., 2008).

Fusion of smaller LDs to form larger LDs is also likely to contribute to LD growth (Guo et al., 2008), and models that implicate SNARE proteins and motor proteins in LD

fusion have been proposed (Boström et al., 2007; Olofsson et al., 2008). A fusion mechanism would alleviate the requirement for phospholipid synthesis during the growth of LDs, because the surface/volume ratio decreases with fusion.

4.4. LDs mobilization

Neutral lipids in LDs are mobilized by lipases to provide metabolic energy (through the oxidation of fatty acids) and lipids for membrane synthesis (Brasaemle, 2007; Ducharme and Bickel, 2008; Zechner et al., 2005). In adipocytes, this lipolysis is triggered by hormonal, nutritional or inflammatory (such as tumor necrosis factor-α) signals.

The fatty acids that are liberated from lipolysis may be activated to acyl-CoA and transported to mitochondria for β-oxidation to provide cellular ATP, may enter the nucleus, where they act as ligands for nuclear hormone receptors and regulate gene transcription, or may be released from the cells to provide fuel or signaling molecules for other cells or tissues.

During lipolysis, LDs might undergo fission, which would dramatically increase the surface area of LDs and enable lipases to better access the neutral-lipid cores. Fission of LDs has been observed in adipocytes after massive lipolytic stimulation (Marcinkiewicz et al., 2006). As the surface area of LDs expands with fission, more surface phospholipids would be required. This requirement might explain why a reduction in phospholipid synthesis through the knockdown of CCT leads to a defect in lipolysis (Guo et al., 2008).

4.5. LDs regression to ER

In contrast to droplets formation, virtually nothing is known about how droplets regress. Most, if not all, cells respond to an excess of free fatty acid or cholesterol by enlarging the number and size of droplets. In turn, droplets disappear under metabolic conditions that consume the stored lipid. Even within the seemingly quiescent droplet, neutral lipids such as cholesteryl esters continuously recycle in a futile pathway that consumes ATP (Brown et al., 1980; McGookey and Anderson, 1983). As the balance shifts towards consumption of lipids, the droplets get smaller and major proteins such as ADRP and perilipin are degraded in the cytosol by the proteasome machinery (Masuda et al., 2006; Xu et al., 2006; Xu et al., 2005). The fate of the integral droplet proteins, by contrast, and the phospholipid monolayer in which they reside is not known. One

possibility is that these elements cycle back to the ER and become part of a ready pool for later droplet formation. A protein that contained an integral LD targeting sequence, as LDIMPs (lipid droplet integral membrane protein), was take like an example.

LDIMPs provide a new conceptual framework for understanding the biogenesis of LDs. These are integral membrane proteins that are inserted into the ER before moving to either endogenous or oleate-induced LDs without exiting the ER in COPII vesicles. In the absence of vesicle traffic, therefore, LDIMPs must reach droplets by moving laterally in the plane of the ER membrane. The hydrophobic targeting signal appears to be specialized for this process. This sequence probably does not span the ER membrane, yet is necessary and sufficient for correct targeting, even when placed in the middle of a protein (Zehmer et al., 2008). Therefore, it is an intrinsic property of these simple hydrophobic sequences to reside in the outer monolayer of the ER and move laterally in the plane of this monolayer before being sequestered by LDs. Several studies have documented that ADRP is degraded by the ubiquitin-proteasome pathway during droplet regression (Masuda et al., 2006; Xu et al., 2006). By contrast, we found that LDIMPs return to the ER where they appear largely to be preserved. This suggests that the phospholipid monolayer surrounding each LD returns to the ER when neutral lipid is depleted. The return of LDIMPs to the ER is essentially the reciprocal of LDIMP movement to existing droplets (Figure). If LDs are always attached to the ER through a thin stalk (Figure b) then LDIMPs can easily return through the stalk. The stalk, in other words, functions as a conduit through which droplet LDIMPs can travel to and from the ER. If, however, LDs do detach from the ER, then LDIMPs must return by monolayer fusion (Figure b) or through transient contact sites (Figure c). Thus, the stalk model is the most parsimonious of the three and can account for both the fate of the monolayer, the return of LDIMPs to the ER and the movement of LDIMPs to existing droplets.

One of the attractive aspects of the LD stalk model is the possibility that phospholipid monolayer stalks function as interorganelle connectors that facilitate the movement of specialized integral membrane proteins and their cargo between different membrane-bound compartments.
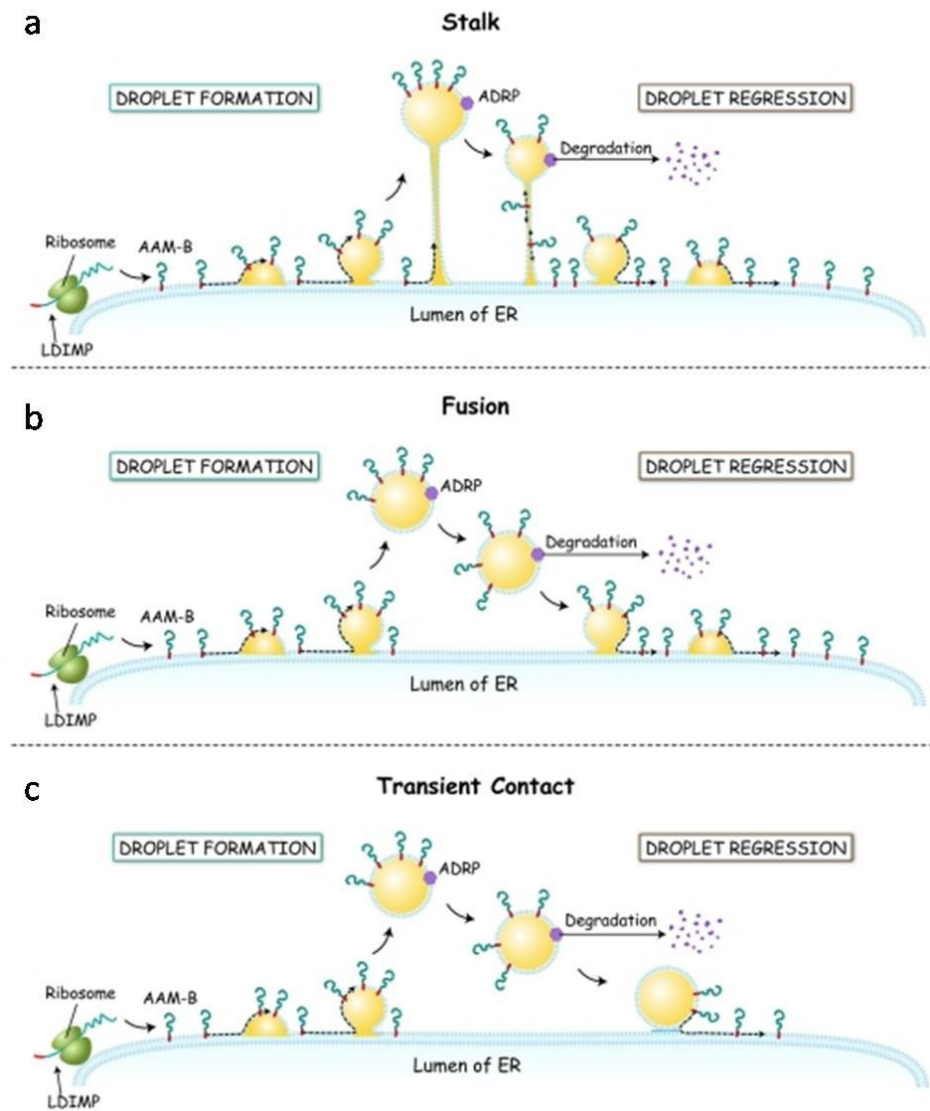
Figure : Three models to explain how integral droplet proteins travel between ER and LD.
(a) Stalk Model. LDIMP proteins such as AAM-B and UBXD8 move from the ER to droplets through a stalk composed of two phospholipid monolayers derived from the ER that remains continuous with LDs. During LD regression, LDIMPs migrate back to the ER through the stalk. (b) Fusion Model. LDIMPs move to form droplets that then bud from the ER to form free LDs. During droplet regression, the LD refuses with the ER and the LDIMPs return to the ER. (c) Transient Contact Model. LDIMPs move into droplets that bud from the ER. During droplet regression, the LD docks with the ER outer monolayer where it delivers the L-DIMP back to the ER without fusing. (*Journal of Cell Science, 2009*)

4.6. LDs interact with other cellular organelles

There is increasing evidence that LDs dynamically interact with other cellular organelles. In particular, LDs are often found in close approximation with the ER, mitochondria, endosomes, peroxisomes and the plasma membrane (Goodman, 2008; Murphy et al., 2008). The functions of these interactions are still largely unknown. These organelle associations might facilitate the exchange of lipids, either for anabolic growth of LDs or for their catabolic breakdown. Alternatively, LDs might provide a means of transporting lipids between organelles within the cell, much like lipoproteins transport lipids between tissues via the blood. Some of the interactions between LDs and other organelles might be mediated and regulated by Rab GTPases, which have been found on LDs (Liu et al., 2008).

Besides storing key lipids, recent studies suggest that LDs might have other functions in cellular physiology or pathology. For example, LDs might act as the protective reservoir for unfolded proteins or other compounds (that are sequestered in the organic phase) to prevent harmful interactions with other cellular components (Ohsaki et al., 2006; Welte, 2007).

The intracellular pathogen *C. trachomatis* induces the accumulation of LDs around the bacteria-replication vacuole and appears to use LD components for replication (Cacchiaro et al., 2008; Kumar et al., 2006). Similarly, the hepatitis C virus appears to use LDs as the platform for viral assembly, and blocking the association of the hepatitis C core protein with LDs impairs viral replication (Miyanari et al., 2007). A better understanding of these LD-pathogen interactions might provide new avenues for therapeutic interventions.

6. METHODS

1. MOLECULAR BIOLOGY TECHNIQUES: GENERATION OF CONSTRUCTS

The REEP1 cDNA was previously obtained from *HeLa cells* RNA extract followed by RT reaction and cloned in the pcDNA3.1/Zeo(+) cloning vector (Qiagen).

1.1. RNA isolation protocol: cells in culture

2. Procedure

- Using at least 10^6 cells, aspirate off the media and wash X1 with ice cold PBS (1-2 ml).
- Aspirate off the PBS (remove as much as possible) and add 1 ml of trizol.
- Scrape the plate briefly, then remove the trizol with a pipette and deposit the trizol/cell lysate into a 1.5 ml eppendorf tube.
- Let sit for 5 min at room temperature.
- Add 250 μl of chloroform and shake the tube vigorously for about 15 seconds.
- Let sit for 5 min at room temp.
- Centrifμge at 10,000 rpm for 5 min.
- At this point, there will be three layers in each tube:
  a. Top layer: clear - aqueous
  b. Middle layer / interphase - white precipitated DNA
  c. Bottom layer - pink organic phase
- Carefully pipette off the aqueous phase. With the larger pipette, it is harder to control the rate and force of fluid withdrawal and this increases the likelihood of drawing some of the organic or DNA phase. Leave behind some of the aqueous phase (about 1 mm above DNA layer to prevent DNA contamination). Place in another 1.5 ml eppendorf.
- Add 550 μl of isopropanol to the aqueous phase and mix gently. Let this sit at room temp for 5 min.
- Centrifuge at maximal speed (14,000 rpm) for 20 min. If a low yield is expected, centrifuge for 30 min.

- Remove and place on ice. There should be a pellet barely visible at the base of each tube. Pour off the isopropanol and add 1 ml of 75% EtOH in DEPC treated H_2O. Mix gently. Recentrifuge at 9500 rpm for 5 min.

- Pour off the EtOH and let the pellets air-dry.

- This is a critical step. If the pellets dry out too long or too much, the RNA crystallizes and is very difficult to resolubilize. If not enough of the EtOH evaporates, this also prevents the RNA from going into solution. After pouring off the bulk of the EtOH wash, there will be approx 30-40 µl left in the bottom of the eppendorf. To quicken the evaporation, centrifuge the tubes briefly to force remaining fluid on the side of the tube to the bottom, then pipette off as much of the EtOH as is feasible. The best time to add DEPC treated water to the RNA pellet is when there is only a tiny meniscus of solution left around the pellet itself.

- Add approx 15-25 µl (depending on yield) of either DEPC treated TE buffer or water to the RNA pellet. To a small eppendorf tube, dilute the RNA 1/40 (1.2 µl in 48.8 µl of TE buffer) and add to a microcuvette (path length = 1 cm). Then measure the absorbance at 260 nm. The 260/280 ratio should be greater than 1.8. If less than 1.5-1.6 or so, the RNA is likely, at least partially degraded. Lower ratios also suggest DNA or thiocyanate contamination. The concentration is essentially the equivalent of the OD at 260 nm (in µg/µl).

3.   **DNAse treatment:**

- The DNAse cocktail consists of the following (per sample):

    > RQ1 Rnase free Dnase: 1 µl
    > Dnase 10x reaction buffer 2 µl
    > DEPC-treated H_2O 6 µl
    > Rnase Out 0.5 µl

- Make a master mix of the above based on the number of RNA samples being treated.

- Prepare the RNA in the following way:
    - Add 2 µg of RNA (calculated by 2 µg/the concentration in µg/µl) to a small eppendorf Bring the total volume of the RNA to 11 µl by adding additional DEPC treated water. (For example, if your RNA concentration is 1 µg/µl, add 2 µl of the RNA to 9 µl of DEPC water).
    - Add 9 µl of the Dnase master mix to the RNA bringing the total volume to 20 µl.s

- This step should be done in a thermal cycler. Incubate the samples at 37°C for 15 min, followed by 65°C for 20 min, then place on ice. Briefly centrifuge each sample to assure all of the volume lies in the bottom of the tube. The DNAase treated RNA can then be used immediately for the reverse transcription reaction.

3.1. Amplification of REEP cDNA

Full-length REEP1 cDNA (606 pb) was obtained by RT-PCR from HeLa cells total RNA.

RT-PCR is short for Reverse Transcription-Polymerase Chain Reaction. RT-PCR is a technique in which a RNA strand is "reverse" transcribed into its DNA complement, followed by amplification of the resulting DNA using a polymerase chain reaction (PCR).

Transcribing a RNA strand into its DNA complement is termed reverse transcription (RT), and is accomplished through the use of a RNA-dependent DNA polymerase (reverse transcriptase). Afterwards, a second strand of DNA is synthesized through the use of a deoxyoligonucleotide primer and a DNA-dependent DNA polymerase. The complementary DNA and its anti-sense counterpart are then exponentially amplified via a polymerase chain reaction (PCR). The original RNA template is degraded by RNase H treatment.

RT-PCR

The complementary strand from RNA template was obtained using the ThermoScript ™ RNase H⁻ Reverse Transcriptase (Invitrogen); for PCR reaction we used Phusion High-Fidelity DNA polymerase (Finnzymes). The entire procedure is described below.

Component	Volume/ 12 ul reaction
Oligo(dT)$_{20}$ (50μM)	1 ul
Total RNA	1 ug
10mM dNTP mix (10 mM each dATP, dGTP, dCTP and dTTP at neutral pH)	1 ul
H$_2$O	add to 12 ul

The misture was incubated at 65°C for 5 minutes and then placed on ice. The contents of the tube was collected by brief centrifugation and to the tube were added:

Component	Volume/ 20 ul reaction
RTBuffer (5X)	4 ul
DTT 0.1M	1 ul
primer Oligo(dT)	1 ul
RNaseOUTTM	1 μl
Superscript III (retrotrascriptase)	200U

Contents of the tube were mixed gently and incubated at 50°C for 60 minutes. The reaction was terminated by heating at 75°C for 5 minutes. To remove the original RNA template, 1μl (2 units) of *E. coli* RNase H was added and incubated at 37°C for 20 minutes.

3.2. Cloning of the HReep cDNA fragment in pcDNA3.1/Zeo(+) plasmid: HReep-HA/pcDNA3.1/Zeo(+), HReep-Myc/ pcDNA3.1/Zeo(+) and HA/HReep-Myc/ pcDNA3.1/Zeo(+)

pcDNA3.1/Zeo(+) is a plasmid designed for high level expression in a variety of mammalian cell lines (see Appendix C, APPENDIX C: PLASMIDS). Three differently tagged REEP1 forms were cloned in the pcDNA3.1/Zeo(+) plasmid: REEP-HA, REEP-Myc and HA-REEP-Myc.

To insert the HA epitope in the N-terminus of REEP, cDNA was amplified from HReep/pDrive vector using the following primers:

Forward

FHAReep1EcorI   5'ctgaGAATTCATGT**ACCCATACGATGTTCCTGACTATGCGGGCGT**GTCATGGATCATCTCCAGGC3'

Reverse

RReep1XhoIStop   5'ctgaCTCGAGCTAGGCGGTGCCTGAGCTGCTAGCGCT3'

To insert the Myc epitope in the C-terminus of HReep, cDNA was amplified from HReep/pDrive vector using the following primers:

Forward

FReep1EcorI   5'ctgaGAATTCATGGTGTCATGGATCATCTCCAGGC3'

Reverse

RReep1XhoI**Myc**   5'ctgaCTCGAG**TTACAGATCTTCTTCAGAAATAAGTTTTTGTTC**GGCGGTGCCTGAGCTGCTAGCGCT3'

To insert the HA epitope in the N-terminal and Myc epitope in the C-terminal of REEP1, cDNA was amplified from HReep/pDrive vector using the following primers:

Forward

FHAReep1EcorI   5'ctgaGAATTCATG**ACCCATACGATGTTCCTGACTATGCGG**
                       GCGTGTCATGGATCATCTCCAGGC3'

Reverse

RReep1XhoIMyc   5'ctgaCTCGAGTTA**CAGATCTTCTTCAGAAATAAGTTTTTG**
                       TTCGGCGGTGCCTGAGCTGCTAGCGCT3'

Primer to clone EGFP in pcDNA 3.1/CT-GFP-TOPO

Fspg31KpnI   ctgaGGTACCATGATCAGCAGCCTGTTTTC

Rspg31XbaI   ctgaTCTAGAGTAGTTTTCCACATCCACATC

To generate each of these three constructs the protocol used was the following:

PCR

Component	Volume/ 50 ul reaction
HReep cDNA (20 μg/ul)	1 ul
Buffer 10X	2 ul
MgCl2 (50mM)	2 μl
dNTPs (10 mM)	0.5 ul
Forward (10 uM)	1 ul
Reverse (10 uM)	1 ul
Taq DNA polymerase (2 U/μl)	0.4 ul
H₂O	add to 50 ul

PCR cycle

Cycle step

Temperature

Time

Initial denaturation

94°C

5 minutes

Denaturation

94°C

30 seconds

Annealing

58°C

30 seconds

Extension

72°C

1 minute

Final extension

72°C

10 minutes

The product of this amplification was inserted in pBSSKII vector.

Restriction reactions

The 5'HReep-Myc-3' fragment was extract from the pBSSKII 5'-HReep-Myc-3' vector by *XBaI* and *EcoRI* enzymatic digestion. pcDNA3.1/Zeo(+) plasmid was linearyzed by *XBaI* and *EcoRI* enzymes pcDNA3.1/Zeo(+) plasmid and HReep-HA or HReep-Myc or HA-HReep-Myc PCR fragments were digested with EcoRI and XhoI restriction enzymes in the following reactions:

Component	Volume/ 50 ul reaction	Component	Volume/ 50 ul reaction
HReep PCR fragment (50ng/ul)	20 ul	pcDNA3.1/Zeo(+) plasmid (100ng/μl)	5 ul
EcoRI (10U/ul)	2 ul	EcoRI (10U/ul)	2 ul
XBaI (10U/ul)	2 ul	XBaI (10U/ul)	2 ul
10X L buffer	5 ul	10X L buffer	5 ul
H₂O	add to 50 ul	H₂O	add to 50 ul

Mixed products were incubated at 37°C for 1 hour and successively separated by electrophoresis through a 1% agarose gel. The bands corresponding to the HREEP PCR fragment and pcDNA3.1/Zeo(+) plasmid were cut from gel and purified using the QIAquick Gel Extraction Kit Qiagen). Purified DNA products were eluted in 10 μl of elution buffer.

The purified DNA fragments were ligated as follows:

Ligation

Component	Volume/ 10 ul reaction
Purified pcDNA3.1/Zeo(+) plasmid (100ng/ul)	3 ul
Purified HReep fragment (50 ng/ul)	6 ul
5X Buffer	3 ul
T4 DNA ligase (1U/ ul) Invitrogen	2 ul
H$_2$O	add to 20 ul

The mixture was incubated at 16°C for 1 hour.

Transformation

Ligation mixture was used for transformation of chemically competent DH5alpha cells (Invitogen). Transformed bacteria were plated on LB–ampicillin agar plates and incubated overnight at 37°C. 10 colonies for each construct were grown in LB medium with ampicillin. Plasmid DNA was successively purified by minipreparation protocol (see Appendix A, Transformation of chemiocompetent cells)and tested by restriction analysis for the right insertion.

Purification of HReep-HA/pcDNA3.1/Zeo(+), HReep-Myc/ pcDNA3.1/Zeo(+) and HA-HReep-Myc/ pcDNA3.1/Zeo(+)

Plasmid DNA were purified from an overnight culture using a "Midi" plasmid purification kit, according to Qiagen Plasmid Midi purification protocols. The final pellets were re-suspended in 50 ul of TE buffer.

3.3. Site specific mutagenesis

To introduce specific nucleotide substitutions in REEP cDNA, site-directed mutagenesis was performed using Pfu Ultra HF DNA polymerase (Startagene).

The basic procedure utilizes a supercoiled double-stranded DNA (dsDNA) vector with an insert of interest and two synthetic oligonucleotide primers containing the desired mutation. The oligonucleotide primers, each complementary to opposite strands of the vector, are extended during temperature cycling by the Pfu Ultra DNA polymerase

polymerase. Pfu Ultra DNA polymerase replicates both plasmid strands with high fidelity and without displacing the mutant oligonucleotide primers. Incorporation of the oligonucleotide primers generates a mutated plasmid containing staggered nicks. Following temperature cycling, the product is treated with DpnI. The DpnI endonuclease (target sequence: 5´-Gm6ATC-3´) is specific for methylated and hemimethylated DNA and is used to digest the parental DNA template and to select for mutation-containing synthesized DNA. DNA isolated from almost all *E. coli* strains is dam methylated and therefore susceptible to DpnI digestion. The nicked vector DNA containing the desired mutations is then transformed into XL1-Blue chemiocompetent cells.

PCR reaction

Component	Volume/ 50 ul reaction
10X PfuUltra HF reaction buffer	5 ul
HReep-HA/pcDNA3.1/Zeo(+) (50 ng/ul) or HReep-Myc/pcDNA3.1/Zeo(+) (50 ng/ul)	1 ul
Forward (10 uM)	1 ul
Reverse (10 uM)	1 ul
10 mM dNTPs	1 ul
Pfu Ultra HF DNA polymerase (2.5 U/ ul)	1 ul
H$_2$O	add to 50 ul

PCR cycle

Cycle step
Temperature
Time
Initial denaturation
95°C
1 minute
Denaturation
95°C

50 seconds

Annealing

52°C

50 seconds

Extension

68°C

10 minutes

Final extension

68°C

30 minutes

Following temperature cycling, the reaction was placed on ice for 2 minutes.
1 μl of the DpnI restriction enzyme (10 U/μl) was added directly to the amplification.
The reaction was mixed by pipetting the solution up and down several times, and
immediately incubated at 37°C for 1 hour to digest the parental (i.e., the non mutated)
supercoiled dsDNA.

Specific primers used for single and multiple substitutions

Aminoacidic Substitutions		Primers In small letters are indicated the substituted nucleotides
P19R	Forward	5'TATTTGGCACCCTTTAC**CGT**GCGTATTATTCCTAC3'
	Reverse	5'GTAGGAATAATACGC**ACG**GTAAAGGGTGCCAAATA3'
A20E	Forward	5'TGGCACCCTTTACCCT**GAG**TATTATTCCTACAAG3'
	Reverse	5'CTTGTAGGAATAATA**CTC**AGGGTAAAGGGTGCCA3'

A132V	Forward	5'TTGAACGTGGCCGTCA**CAG**CGGCTGTGATG3'
	Reverse	5'CATCACAGCCGCTGT**GAC**GGCCACGTTCAA3'

Transformation

10 μl of each reaction mixture was used for transformation of chemically competent XL1-blue bacteria. Transformed bacteria were plated on LB–ampicillin agar plates and incubated overnight at 37°C.

10 colonies were grown in LB medium with ampicillin. Plasmid DNA was successively purified by minipreparation protocol (see Appendix A, APPENDIX A: GENERAL PROTOCOLS for procedure).

Plasmid purification

Plasmids were purified from an overnight culture using a "Midi" plasmid purification kit, according to Qiagen Plasmid Midi purification protocols. The final pellets were re-suspended in 50 ul of TE buffer.

Sequencing of mutated REEP1 cDNA

Two clones of each construct have been sequenced to verify the presence of the specific mutations. The DNA clones were sequenced by Bio-Fab Research (http://www.biofabresearch.it/index2.html) using the following primers:

T3 universal primer	5'AGCACCTGCAGCTCTTCACT3'
T7 universal primer	5'TAATACGACTCACTATAGGG3'

4. CELLULAR BIOLOGY

4.1. Cells culture

HeLa cell culture was derived from a cervical carcinoma of a 31 years old african-american woman. This was the first aneuploid line derived from human tissue maintained in continuous cell culture.

Cos7 cell line was obtained by immortalizing a CV-1 cell line derived from kidney cells of the African green monkey with a version of the SV40 genome that can produce large T antigen but has a defect in genomic replication.

HepG2 is a perpetual cell line which was derived from the liver tissue of a 15 years old Caucasian American male with a well differentiated hepatocellular carcinoma.

4.1.1. Propagation and subculturing

HeLa, Cos7 and HepG2 cells were grown in complete DMEM medium (see Appendix B, APPENDIX B: STOCKS AND SOLUTIONS) with 10% FBS serum and antibiotics, at 37°C in a CO_2 incubator.

Cells were passaged when growing logarithmically (at 70 to 80 % confluency) as follows:

- The cell layer was briefly washed twice with PBS to remove all traces of serum, then trypsin solution (see Appendix B, APPENDIX B: STOCKS AND SOLUTIONS) was added to flask and cells were observed under an inverted microscope until cell layer was dispersed (usually within 5 minutes).

- Complete growth medium was added to stop trypsin action, cells were aspirated by gently pipetting and diluted 1:10 into a new flask with new complete medium.

- For cell count, an aliquot of the cell suspension, before plating, was mixed 1:1 with a solution of 0.1% Trypan blue (Sigma) in PBS. Trypan blue is a vital stain used to selectively colour dead cells. In a viable cell Trypan blue is not absorbed, however it traverses the membrane in a dead one. Hence, dead cells are shown as a distinctive blue colour under a microscope. 10 ul of the above mixture was charged on a counting chamber and viable cells in the "counting squares" were counted. The cells density was calculated as follows: average of counted cells/ counting square X 10^4 X dilution factor (=2) = number of cells/ml.

4.2. Plasmid DNA Transfection

To introduce expression plasmids into HeLa, Cos7 and HepG2 cells *TransIT-LT1*® Transfection Reagent (Mirus) was used. Transfection Reagent is a mix of cationic lipids. The basic structure of cationic lipids consists of a positively charged head group and one or two hydrocarbon chains. The charged head group governs the interaction

between the lipid and the phosphate backbone of the nucleic acid, and facilitates DNA condensation. The positive surface charge of the liposomes also mediates the interaction of the nucleic acid and the cell membrane, allowing for fusion of the liposome/nucleic acid ("transfection complex") with the negatively charged cell membrane. The transfection complex is thought to enter the cell through endocytosis. Once inside the cell, the complex must escape the endosomal pathway, diffuse through the cytoplasm, and enter the nucleus for gene expression.

Protocol

In a six-well, one day before transfection, 2×10^5 cells were plated in 1,5 ml of DMEM medium without antibiotics so that cells were 90-95% confluent at the time of transfection.

For each transfection sample, the complexes were prepared as follows:

- DNA (2-3ug) was diluted in 250 µl of DMEM medium without antibiotics and serum and mixed gently.

- *TransIT-LT1* was mixed gently before use, then 8ul were diluted in 250 µl of DMEM medium without antibiotics and serum. The sample was incubated for 5 minutes at room temperature.

- After the 5 minute incubation, the diluted DNA was combine with the diluted *TransIT-LT1* (total volume = 500 µl), mixed gently and incubated for 20 minutes at room temperature.

The 500 µl of complexes were added to each well containing cells and medium.

Cells were incubated at 37°C in a CO_2 incubator for 24 hours prior to testing for transgene expression.

4.3. Immunocytochemestry (ICC)

For immunocytochemistry, the day before transfection cells were plated on a glass coverslip previously sterilized with ethanol.

The procedure used is divided into the below steps:

Fixation

One day after transfection, the cells were fixed in 4% paraformaldehyde in PBS pH 7.4 for 10 minutes at room temperature. The cells were then washed tree times with PBS to eliminate paraformaldehyde.

Permeabilization

To permeabilize cell membranes and improving the penetration of the antibody, the cells were incubated for 10 minutes with PBS containing 0.1% Triton X-100 (Applichem).

Blocking and Incubation

Cells were incubated with 10% serum in PBS for 10 minutes to block non specific binding of the antibodies.

Primary antibodies, diluted in PBS with 5% serum, were applied for 1 hour in a humidified chamber at 37°C. Cells were washed three times with PBS and then secondary antibodies, diluted in PBS, were applied for 1 hour in a humidified chamber at 37°C.

Mounting and analysis

Coverslips were mounted with a drop of the mounting medium Mowiol (Sigma). Images were collected with a Nikon C1 confocal microscope and analysed using either Nikon EZ-C1 (version 3.7) or NIH ImageJ (version 1.32J) softwares.

Primary antibodies used	Dilution
Anti REEP1 rabbit (Proteintech Europe)	1:200
Anti c-Myc rabbit (Sigma)	1:200
Anti HA rabbit (Sigma)	1:200
Anti c-Myc mouse (Sigma)	1:200
Anti HA mouse (Sigma)	1:200
Anti calnexin rabbit (Santa Cruz Biotechnology)	1:200
Anti PDI mouse (BD biosciences)	1:100
Anti GM130 mouse (BD biosciences)	1:200
Anti-ubiquitin rabbit (Chemicon)	1:200
Anti GM130 mouse (BD biosciences)	1:200

Primary antibodies used	Dilution
Anti apo-B100 rabbit (Calbiochem)	1:100
Anti-GFP mouse (Sigma A*ldrich*)	1:200
Anti LAMP2 rabbit (Sigma A*ldrich*)	1:100
Anti-ALDI rabbit (Acris Antibody)	1:100

Secondary antibodies used	Dilution
DyLight™488 anti rabbit (Jackson Immuno Research)	1:1000
DyLight™488 anti mouse (Jackson Immuno Research)	1:1000
Cy™3 anti mouse (Jackson Immuno Research)	1:1000
DyLight™549 anti rabbit (Jackson Immuno Research)	1:1000
DyLight™649 anti mouse (Jackson Immuno Research)	1:1000
DyLight™649 anti rabbit (Jackson Immuno Research)	1:1000

Markers	Dilution
BODIPY 493/503 (Invitrogen)	1:1000
Mito Tracker Orange CMTMRos (Invitrogen)	1:1000

7.

1.1. Selective membrane permeabilization

To determine the right REEP1 membrane topology by a selective membrane permeabilization, the sample were prepared like a normal ICC (Methods, Immunocytochemestry (ICC)), excluding the permeabilization part, that was performed as follows:

- After paraformaldehyde fixation, one slide was treated like a common ICC assay (Methods,Immunocytochemestry (ICC)), while the others were sequentially processed with digitonin (20μM) for 2 minutes, a saponin that used for this timespanning and in these concentrations permeabilized only the cellular membrane, but not the organels membrane. One slide was mounted and analized.

- The other two slides were treated with trypsin (0,25% for 2 minutes), a proteolitic enzyme that selectively cutted the Arg-Lys bonds. If a protein has C or N terminal part face cell cytoplasm, in this time was cutted off. One of two slide was mounted and analized.

- The last one slide was treated with a solution of Triton X-100 0.1% (Applichem); triton is a surfactant that permeabilized, in this case, the organels membrane. The slide was mounted and analized.

- 24h before, the cells were trasfected with REEP1-GFP (Methods, Plasmid DNA Transfection) construct by *TransIT-LT1*: GFP tag was in the N-terminal part of the construct. The slides were immunostained with anti-GFP antibody and anti-PDI, an ER lumenal-specific marker used as a control of successful selective membranes permeabilization.

1.2. Inhibition of proteasomal pathway

The proteasomal pathway was inhibited by use a specific inhibitor, ALNN (*N*-acetyl-l-leucinyl-l-leucinyl-l-norleucinal).

- In a six-well plate, one day before transfection with REEP1-Myc construct, 2 x 10^5 Cos7 cells were plated in 1,5 ml of DMEM medium without antibiotics; the culture medium was added of a mix of oleic and linoleic acid (200Mm).

- 3h before fixation, the cells were treated with ALNN 10μM.

- So, the analysis proceeded with a ICC (Methods, Immunocytochemestry (ICC)).

- The slides were immunostained with anti-Myc and anti-ApoB100 antibody ApoB-100 is a lipoprotein that was degradated by proteasomal pathway.

1.3. Inhibition of autophagy

The authophagy pathway was inhibited by use a specific inhibitor, 3-methyladenine (3-MA).

- In a six-well plate, one day before transfection with REEP1-Myc construct, 2 x 10^5 Cos7 cells were plated in 1,5 ml of DMEM medium without antibiotics; the culture medium was added of a mix of oleic and linoleic acid (200Mm).

- 3h before fixation, the cells were treated with 3-MA 10μM.

- So, the analysis proceeded with a ICC (Methods, Immunocytochemestry (ICC)). The slides were immunostained with anti-Myc and anti-Lamp2 antibody Lamp2 is a protein that was degradated by authophagy.

1.4. Droplet regression experiments

Cos7cells were grown to ~60% confluence on glass coverslips. The cells were transfected with cDNA using using *TransIT-LT1* (Mirus) according to the manufacturer's protocol according to the manufacturer's protocol and then incubated for an additional 3 hours.

The medium was then replaced with complete medium containing 1 mg/ml BSA and 100 μM oleic acid and cultured for 6 hours. One set of coverslips was fixed and stored in PBS at 4°C.

The medium on the remaining cells was replaced with complete medium containing 1 mg/ml BSA, 50 μg/ml cycloheximide and 7.5 μM triacsin C and the cells were incubated for further 15 hours. The remaining cells were fixed and all coverslips were processed for immunofluorescence.

2. BIOCHEMICAL TECHNIQUES

2.1. Co-Immunoprecipitation (Co-IP)

Co-immunoprecipitation (Co-IP) is a common technique for protein interaction discovery.

An antibody for the protein of interest, linked to a support matrix, is incubated with a cell extract so that the antibody will bind the protein in solution. The antibody/antigen complex will then be pulled out of the sample: this physically isolate, from the rest of the sample, the protein of interest and other proteins potentially bound to it. The sample can then be separated by SDS-PAGE for Western blot analysis.

In Co-IP experiments, anti-Myc agarose conjugate (Sigma) was used. Anti-c-Myc agarose conjugate is prepared with an affinity purified anti-c-Myc antibody coupled to cyanogen bromide-activated agarose. The purified antibody is immobilized at 1.0 to 1.5

mg antibody per ml agarose. Anti-c-Myc antibody is developed in rabbit using a peptide corresponding to amino acid residues 408-425 of human c-Myc as the immunogen. Anti-c-Myc antibody recognizes the epitope located on c-Myc tagged fusion proteins and it reacts specifically with N- and C- terminal c-Myc-tagged fusion proteins.

The co-immunoprecipitation procedure used is the following:

- 10^6 cells, plated on a six wells plate, were harvested using 0.5% Triton X-100 (Applichem) in PBS, incubated in ice for 15 minutes and then centrifuged at 16000g for 15 minutes.

- 30 ul of anti-c-Myc agarose conjugate suspension was added to a microcentrifuge tube and washed 5 times with PBS by a short spin.

- Cell extract (lysate) was added to the resin and incubated for 2 hours on an orbital shaker at room temperature.

- At the end of incubation time, the supernatant was recovered and the resin was washed 5 times with PBS.

- After the final wash, 70 ul of 1X Laemmli buffer (see Appendix B, APPENDIX B: STOCKS AND SOLUTIONS) were added to the resin and incubated at 95°C for 5 minutes.

- After boiling, the sample was vortexed and then centrifugated for 5 seconds (pellet).

- The presence of the c-Myc tagged protein and of other proteins potentially bound to it was detected in lysate, supernatant and pellet by Western blotting.

2.2. Immunoisolation of membrane vesicles and membrane fractionation

To obtain harbouring vesicles, the sample were prepared as follows:

- 10^6 transfected cells, plated on a six wells plate, were suspended in homogenization buffer (10 mM HEPES-KOH buffer pH 7.4 containing 0.22 M mannitol, 0.07 M sucrose and protease inhibitors) and homogenized using a syringe with a 26-gauge needle.

- Homogenate was sonicated and the supernatant containing vesiculated membranes recovered by centrifugation at 4000g for 5 minutes at 4°C in order to remove unbroken organelles.

- When required, the vesiculated membranes were mixed with another pool of harbouring vesiscles and incubated at 30°C for 1 hour.

- After incubation, immunoprecipitation of the harbouring vesicles was performed as described above (Co-Immunoprecipitation).

- The remaining supernatants containing vesiculated membranes were centrifugated at 120000 g for 60 minutes to separate a membrane fraction (pellet) and a soluble fraction (supernatant).

- Supernatant and pellet derived from the immunoprecipitation and 100000 g centrifugation were analysed by western blotting.

2.3. REEP1 Membrane topology by membrane fractionation

To determine the right REEP1 membrane topology the sample was initially prepare like above (chapter 1.3.2) and when we arrived at the second one point the experiment proceeded in this way:

- The membrane fraction (pellet) was resuspended in homogenization buffer.

- The sample was divided into three parts: one part was caricated directly in blot, while the others parts were incubated at 37°C for 15 minutes after one sample were added of proteinase K, that cut all the protein part that was revolt to the cytoplasmatic part.

- All the samples were analysed by western blotting.

2.4. Immunoisolation of Lipid Droplets (LDs)

- HepG2 cells were trasfected with cDNA using *TransIT-LT1*(Mirus) according to the manufacturer's protocol then incubated for 24h in a medium added of oleic and linoleic acid 100μM

- The cells were scraped into PBS containing 200μM PMSF.

- After centrifugation pellet was resuspended in 800μl buffer A (250 mM sucrose, 20 mM Tris-HCl, pH 7.4) and incubate on ice for 20 minutes.

- The cells were broken by five passes through a 22 G needle.

- A PNS was prepared by centrifugation at 1000g for 7 minutes.

- The PNS was layered on top of 300 μl of cushion buffer 1 and centrifuged for 30 minutes at 100000g in a TLA55rotor.

- The supernatant (excluding the cushion) was transferred to a fresh tube and the droplets were floated to the top by centrifugation at 10000g for 4 minutes.

- The underlying cytosol was recovered to a fresh tube using a gel-loading tip until droplets drawn from the top reached the bottom of the tube. This process was repeated until 100 μl of fluid remained.

- The remaining sample was overlaid with 300 μl buffer B (100mM KCl, 2 mM MgCl$_2$, 20mM HEPES, pH 7.4) and centrifuged for a final time.

- 150 μl of the underlying fluid was removed and discarded leaving partially purified droplets.

- The cushion from the 100000g centrifugation was discarded and the total membrane pellet was washed with buffer A and then resuspended in 100 μl buffer A.

- All samples were precipitated by addition of 100% acetone followed by centrifugation at 20800g for 10 minutes.

- The pellets were resuspended in sample buffer and boiled for 5 minutes.

- Droplets, total membrane and cytosol were separated by PAGE and then analyzed by immunoblotting.

2.5. SDS PAGE

SDS-PAGE stands for Sodium dodecyl sulfate (SDS) polyacrylamide gel electrophoresis (PAGE) and is a method used to separate proteins according to their size. Since different proteins with similar molecular weights may migrate differently due to their differences in secondary, tertiary or quaternary structure, SDS, an anionic detergent, is used in SDS-PAGE to reduce proteins to their primary (linearized) structure and coat them with uniform negative charges: proteins having identical charge to mass ratios are fractionated by size.

Gel making

The resolving gel was prepared with a 10% polyacrylamide content, while the stacking gel had a 5% acrylamide concentration.

Components	Resolving gel	Stacking gel
Acrylamide solution (Fluka)	10% (v/v)	5% (v/v)

Tris-HCl pH 8.8	0.37M	
Tris-HCl pH 6.8		0.125M
Ammonium persulphate	0.1% (w/v)	0.1% (w/v)
SDS	0.1% (w/v)	0.1% (w/v)
TEMED	0.02% (v/v)	0.02% (v/v)

Sample preparation

Samples were diluted in Laemly buffer (Appendix B) and then boiled at 95°C for 5 minutes.

Running the electrophoresis

The amperage applied was 15mA/gel until the proteins reached the resolving gel, then it was increased to 25mA/gel.

Western blotting

After the electrophoresis, the proteins were transferred from gel to PVDF membrane (Amersham Biosciences).

The membrane was blocked with a solution of 10% milk in TBS-T (APPENDIX B: STOCKS AND SOLUTIONS) for 15 minutes at room temperature on a shaking platform.

The membrane was then incubated with the primary antibody diluted to the appropriate concentration in TBS-T and milk 2%, at 4°C O/N.

The secondary antibody diluted to the appropriate concentration in TBS-T was added and incubated for 1 hour at room temperature.

The membrane detection was performed by ECL plus kit (Amersham Biosciences).

Primary antibodies used	**Dilution**

Anti c-Myc mouse (Sigma)	1:1000
Anti HA mouse (Cell Signalling)	1:1000
Anti PDI mouse (BD biosciences)	1:500
Anti calnexin rabbit (Millipore)	1:1000
Anti caveoline rabbit (Abcam)	1:1000
Anti-α-actin mouse (sigma)	1:1000

Secondary antibodies used	**Dilution**
Anti mouse-HRP (Dako)	1:10000
Anti rabbit-HRP (Dako)	1:10000

8.   APPENDIX A: GENERAL PROTOCOLS

1.1. Transformation of chemiocompetent cells

- Gently thaw the chemiocompetent cells on ice.

- Add ligation mixture to 50 μl of competent cells and mix gently. Do not mix by pipetting up and down.

- Incubate on ice for 30 minutes.

- Heat-shock the cells for 30 seconds at 42°C without shaking.

- Immediately transfer the tube to ice.

- Add 450 μl of room temperature S.O.C. medium.

- Cap the tube tightly and shake the tube horizontally (200 rpm) at 37°C for 1 hour.

- Spread 20 μl and 100 μl from each transformation on prewarmed selective plates and incubate overnight at 37°C.

1.2. Preparation of plasmid DNA by alkaline lysis with SDS: minipreparation

Plasmid DNA may be isolated from small-scale (1-3 ml) bacterial cultures by treatment with alkali and SDS.

- Inoculate 3 ml of LB medium (APPENDIX B: STOCKS AND SOLUTIONS) containing the appropriate antibiotic with a single colony of transformed bacteria. Incubate the culture overnight at 37°C with vigorous shaking.

- Pour 1.5 ml of the culture into a microfuge tube. Centrifuge at maximum speed for 30 seconds in a microfuge. Store the unused portion of the original culture at 4°C.

- When centrifugation is complete, remove the medium by aspiration, leaving the bacterial pellet as dry as possible.

- Resuspend the bacterial in 100 μl of ice-cold Alkaline lysis solution I (Appendix B, APPENDIX B: STOCKS AND SOLUTIONS) by vigorous vortexing.

- Add 200 μl of freashly prepared Alkaline lysis solution II (APPENDIX B: STOCKS AND SOLUTIONS) to each bacterial suspension. Close the tube tightly, and mix the contents by inverting the tube rapidly five time. Do not vortex. Store the tube on ice.

- Add 150 μl of ice-cold Alkaline lysis solution III (APPENDIX B: STOCKS AND SOLUTIONS). Close the tube and disperse Alkaline lysis solution III through

the viscous bacterial lysate by inverting the tube several times. Store the tube on ice 3-5 minutes.

- Centrifuge the bacterial lysate at maximum speed for 5 minutes at 4°C in a microfuge. Transfer the supernatant to a fresh tube.

- Precipitate nucleic acids from the supernatant by adding 2 volumes of ethanol at room temperature. Mix the solution by vortexing and then allow the mixture to stand 2 minutes at room temperature.

- Collect the precipitate of nucleic acid by centrifugation at maximum speed for 10 minutes at 4°C in a microfuge.

- Remove the supernatant by gentle aspiration. Stand the tube in an inverted position on a paper towel to allow all of the fluid to drain away. Use a pipette tip to remove any drops of fluid adhering to the walls of the tube.

- Add 2 volumes of 70% ethanol to the pellet and invert the closed tube several times. Recover the DNA by centrifugation at maximum speed for 5 minutes at 4°C in a microfuge.

- Again remove all the supernatant by gentle aspiration.

- Dissolve the nucleic acids in 50 ul of TE buffer (pH 8.0) or distillated autoclavated water containing 20 ug/ml DNase-free RNase A (pancreatic RNase). Vortex the solution gently for a few seconds. Store the DNA solution at -20°C.

9.   APPENDIX B: STOCKS AND SOLUTIONS

LB Medium (Luria-Bertani Medium)

Bacto-tryptone	10g
Yeast extract	5g
NaCl	10g
H_2O	to 1 Liter

Autoclave.

LB Agar

Bacto-tryptone	10g
Yeast extract	5 g
NaCl	10 g
Agar	20g
H_2O	to 1 Liter

Adjust pH to 7.0 with 5 N NaOH. Autoclave.

LB–Ampicillin Agar

Cool 1 Liter of autoclaved LB agar to 55° and then add 10 ml of 10 mg/ml filter-sterilized Ampicillin. Pour into petri dishes (~25 ml/100 mm plate).

SOC medium

Bacto-tryptone	20g
Yeast extract	5 g
NaCl	0,5 g
KCl 1M	2,5 ml
H_2O	to 1 Liter

Adjust pH to 7.0 with 10N NaOH, autoclave to sterilize, add 20 ml of sterile 1 M glucose immediately before use.

Alkaline lysis solution I

Glucose 50 mM
Tris HCl 25 mM (pH 8.0)
EDTA 10 mM (pH 8.0)

Solution I can be prepared in batches of approximately 100 ml, autoclaved for 15 minutes and stored at 4 °C.

Alkaline lysis solution II

NaOH 0.2 N (freshly diluted from a 10 N stock)
SDS 1% (w/v)

Alkaline lysis solution III

Potassium acetate 3 M
Glacial acetic acid 11.5% (v/v)

TE Buffer

Tris-HCl 10 mM (pH 7.5)
EDTA 1 mM

DMEM complete medium

DMEM 4.5g/L Glucose with L-Glutamine (Lonza)
FBS 10% (v/v)
Penicillin-Streptomycin mixture 100X (Lonza, contains 5000 units potassium penicillin and 5000

ug streptomycin sulfate).

Phoshate Buffered Saline (PBS)

KH_2PO_4	1444 mg/L
NaCl	9000 mg/L
Na_2HPO_4	795 mg/L

Trypsin solution

Trypsin 2,5% 10X (Lonza)

Running buffer 1X

Tris 25mM
Glycine 250mM
SDS 0.1%
In deionized H_2O

Transfer buffer 1X

Tris 25mM
Glycine 192mM
In deionized H_2O

TBS-T buffer 1X

Tris 100mM
NaCl 1,5M
Tween-20 1%
In deionized H_2O

Laemmli buffer 2X

SDS 4%
Glycerol 20%

2-mercaptoethanol 10%
Bromphenol blue 0,004%
Tris HCl 125mM
The solution has a pH of approximately 6.8.

10.   APPENDIX C: PLASMIDS

1.1. pDrive cloning vector (Qiagen)

The pDrive Cloning Vector provides superior performance through UA-based ligation and allows easy analysis of cloned PCR products.

This vector allows ampicillin and kanamycin selection, as well as blue/white colony screening. The vector contains several unique restriction endonuclease recognition sites around the cloning site, allowing easy restriction analysis of recombinant plasmids.

The vector also contains a T7 and SP6 promoter on either side of the cloning site, allowing *in vitro* transcription of cloned PCR products as well as sequence analysis using standard sequencing primers. In addition, the pDrive Cloning Vector has a phage f1 origin to allow preparation of single-stranded DNA (Figure).

1.2. pcDNA3.1/Zeo(+) (Invitrogen)

pcDNA3.1/Zeo (+) is an expression vector, derived from pcDNA3.1, designed for high-level stable and transient expression in a variety of mammalian cell lines.

To this aim, it contains Cytomegalovirus (CMV) enhancer-promoter for high-level expression; large multiple cloning site; Bovine Growth Hormone (BGH) polyadenylation signal; transcription termination sequence for enhanced mRNA stability and Zeocin resistance coding region (Figure).

Figure : pDrive Cloning vector map

pcDNA3.1/Zeo(+)   Code: PMC 006

Comments for pcDNA3.1/Zeo (+)
5015 nucleotides

CMV promoter: bases 209-863
T7 promoter priming site: bases 863-882
Multiple cloning site: bases 895-1010
BGH reverse priming site: bases 1022-1039
BGH polyadenylation signal: bases 1021-1235
f1 origin: bases 1298-1711
SV40 promoter and origin: bases 1776-2101
EM7 promoter: bases 2117-2183
Zeocin™ resistance gene: bases 2184-2558
SV40 polyadenylation: bases 2688-2817
pUC origin: bases 3201-3874 (C)
bla promoter: bases 4880-4978 (C)
Ampicillin (*bla*) resistance gene: bases 4019-4879 (C)

pcDNA3.1/Zeo, a mammalian
expression vector derived from
pcDNA3.1, contains CMV promoter
and Zeocin resistance coding gene
and allows high-level stable and
transient expression in mammalian
cells.

For local research purposes only

اهدایی دکتر عزیزی

Ncol	Sall
3463	2793
1352	2222
220	

Figure : pcDNA3.1/Zeo(+) map

11.   RESULTS

1.   REEP1 localizes to the ER

In order to get an insight on the biological role of REEP1, we investigated its subcellular expression by transiently transfecting different epitope-tagged REEP1 constructs in Cos7 cells (Figure); the cells expressing REEP1-Myc (Figure a), REEP-HA (Figure b) and HA-REEP-Myc (Figure c) were fixed and stained with antibodies that recognize Myc and HA epitope tags (Methods Immunocytochemestry (ICC)). Furthermore, the use of different epitopes (HA versus Myc) either positioned at the N- or C-terminus did not change REEP1 localization. Immunofluorescence studies showed that REEP1 protein localize to a reticular structures resembling endoplasmic reticulum (ER) membranes.

Double immunofluorescence experiments using REEP1-Myc construct and appropriate markers recognizing ER, Golgi apparatus, microtubules and mitochondria are analyzed by confocal microscopy, Cos7 cells expressing REEP1-Myc were fixed and stained with antibodies anti-GM130 to visualize Golgi apparatus, anti-β-tubulin as a marker to microtules network, mitotracker that recognizes mitochondria and anti-Myc tag to show REEP1 expression. To visualized ER membrane we used Atlastin-GFP construct generated fusing Atlastin, an integral protein of ER, and GFP (Green Fluorescente Protein) Merged images showed no overlap between REEP1-Myc and Golgi apparatus, mitochondria or microtubules proteins (Figure) but a complete co-localization with ER marker, Atlastin.

Sequence inspection suggests that REEP1 protein, as well as other REEPs family member, was a polytopic membrane-spanning protein with a high proportion of hydrophobic residues. In Figure , is possible to show a hydropathy plot of REEP1aminoacid sequence; based on this plot, REEP1 is predicted to contain at least two putative transmembrane segments, depicted by two peak regions of hydrophobicity.

As a second step in these studies, we documented the ER membrane association of REEP1 by transfecting Cos7 cells with REEP1-Myc. Transfected cells are homogenize in the absence of detergent and fragmented membranes are vesciculated by sonication. Fractionation of cleared cell homogenates showed that REEP1 and the ER resident integral protein calnexin partitioned exclusively to the membrane fraction

(Figure). This demonstrates that REEP1 remained properly associated with ER membranes and, in particularly that is an integral membrane protein associated to the ER.
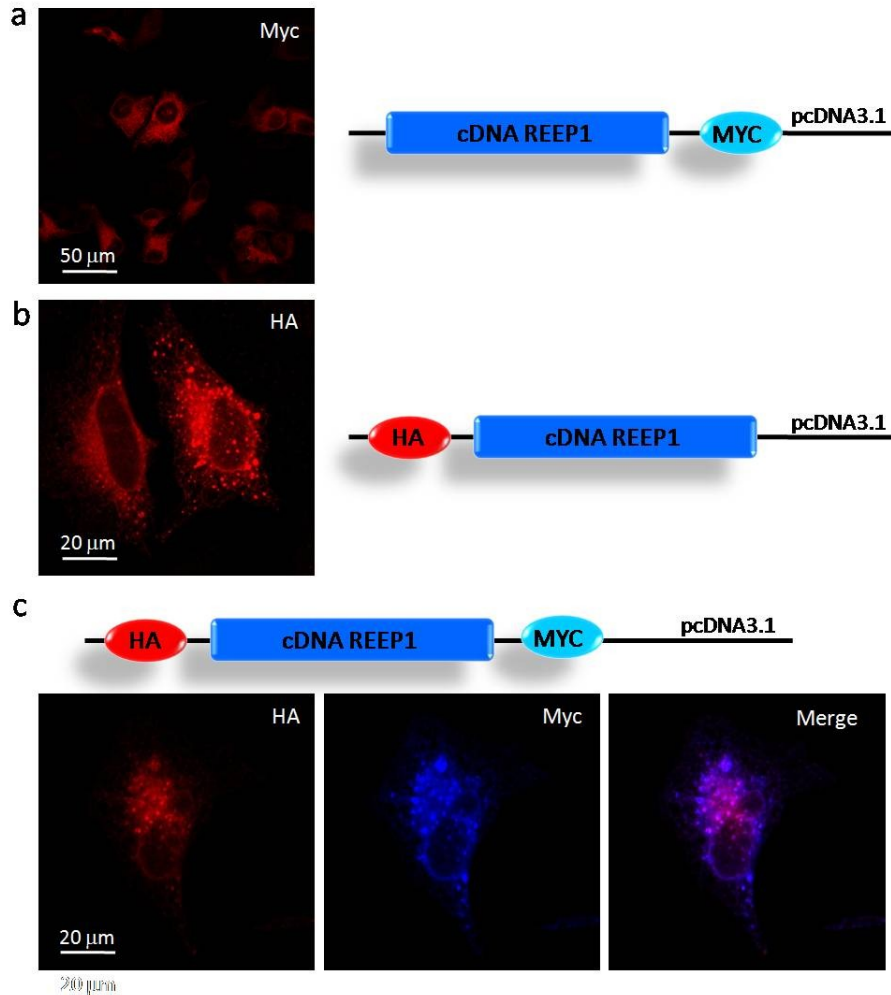
Figure : REEP1 expression in Cos7 cells.
Cos7 cells were transfected with (a) cDNA encoding C-terminally Myc-tagged REEP1; (b) cDNA encoding N-terminally HA-tagged REEP1 and (c) cDNA encoding N-terminally HA-tagged and C-terminally Myc-tagged REEP1. The cells were fixed and processed for indirect immunofluorescence localization of (a) Myc (red); (b) HA (red) and (c) both HA (red) and Myc (blue). Scale bars: 50 μm (a) or 20 μm (b, c). Relative schemes of constructs used are represented.
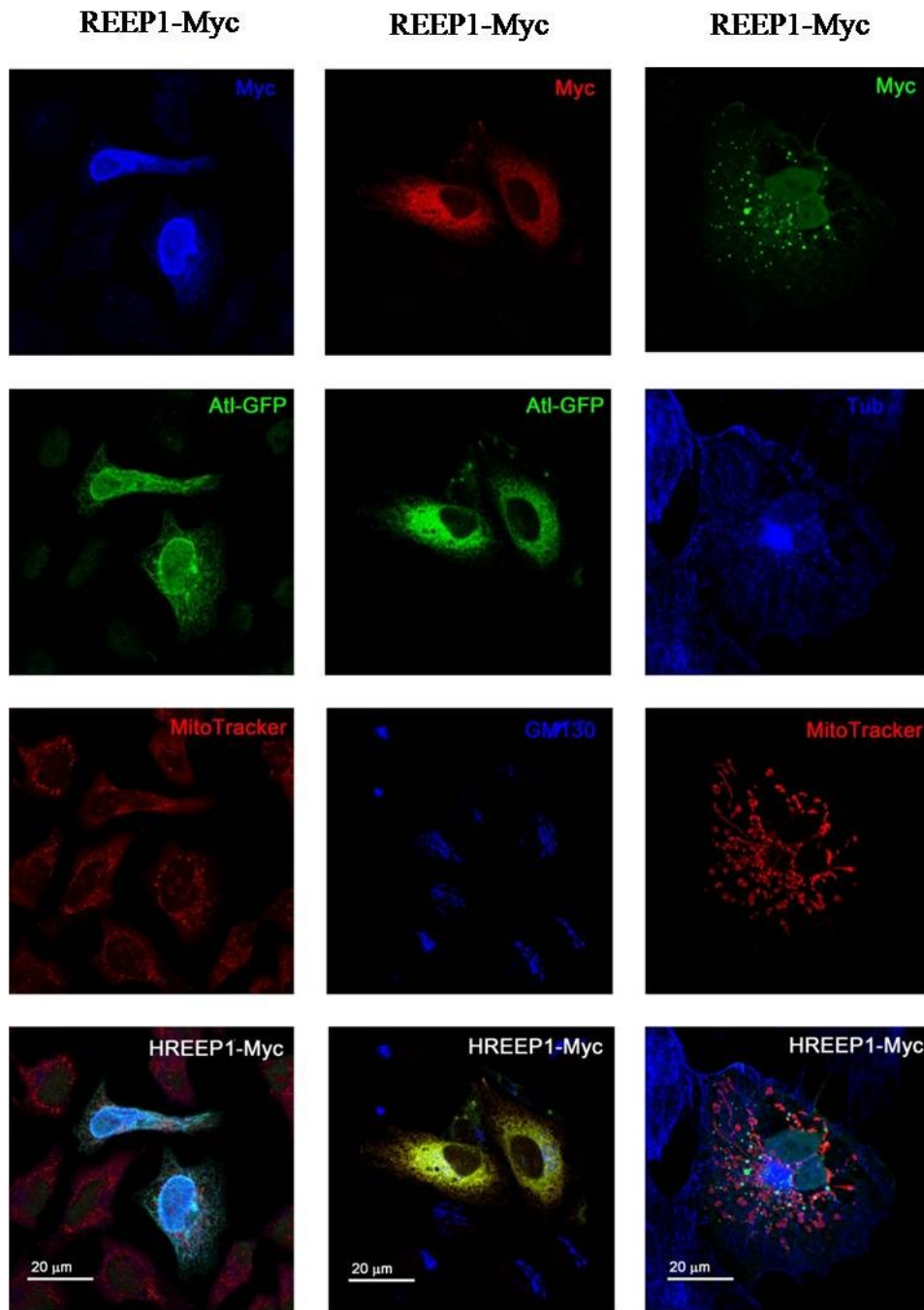
Figure : REEP1-Myc localizes on ER membranes.
Cos7 cells coexpressing Myc-tagged REEP1 (blue) and ATL-GFP (green) to visualize ER, costained for the mitochondrial marker Mitotracker (red) (left column); Cos7 cells coexpressing Myc-tagged REEP1 (red) and ATL-GFP (green) co-stained for the *cis/medial*-Golgi maker GM130 (blue) (central column) and Cos7 cells expressing Myc-tagged REEP1 (green) costained for microtubules antibody β tubuline (blue) and for the mitochondrial marker Mitotracker (red) (right column). Scale bars: 20 μm.
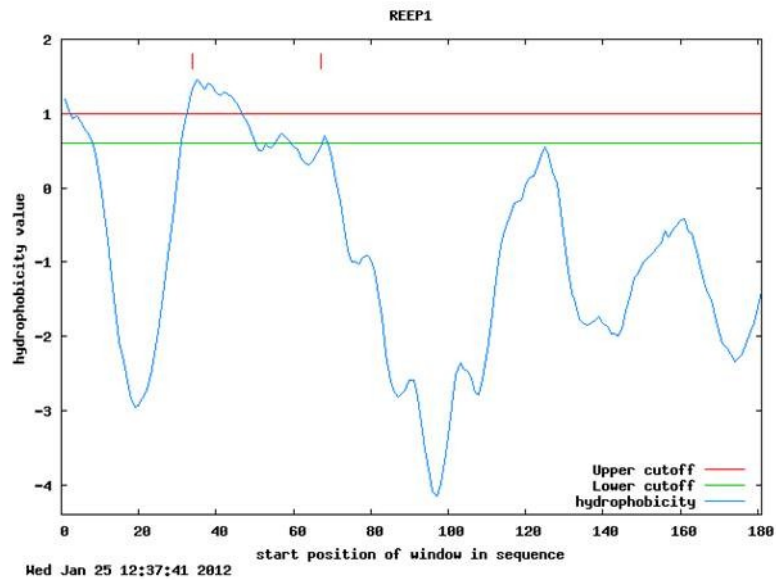
Figure : Hydropathy plot and predicted membrane topology of human REEP1.
Hydropathy plot of REEP1. The residue-specific hydropathy index was calculated over a window of 18 residues by the method of Kyte and Doolittle using software from TopPRED.

a

b
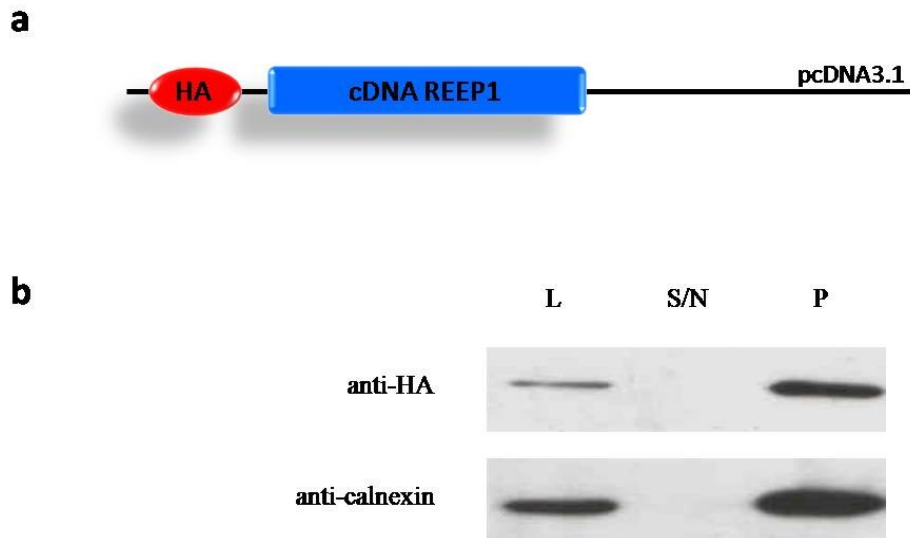
Figure : REEP1 is an integral membrane protein associated with the ER.
Cos7 cells were trasfected with REEP1-HA construct represents above (a); (b) the cells were lysate by sonication (L), centrifuged, the supernatant was recuperated (S/N) and the pellet (P) was resuspended in an appropriate buffer. The samples are analyzed by western blotting; each preparation was immunoblotted with anti-HA antibody to detect REEP1 and anti-calnexin antibody to detect the ER. The immunoisolation of membrane vesicles reveals that REEP1 protein is an integral membrane protein associated to the ER.

2. HREEP1[P19R] localizes around lipid droplets (LDs).

The most common types of REEP1 alterations in HSP patients are small frameshift mutations (that lead to pre-terminal stop codons); destruction of canonical splicing motives (that usually results in frameshifts and pre-terminal stops); missense mutations (an aminoacid replacement); micro-RNA target site alterations and large duplications. Mutations in REEP1 identified to date are listed in Table (Beetz et al., 2008, Slang et al., 2008).

Sequence variation	Exon	Intron	Predicted effect on splicing	Effect on protein	Creation of alternative stop codon
c.-1delCAT	1		None	p.M1fs	Yes
c.49delC	2		None	p.L17fs	Yes
c.56C>G	2		None	p.P19R	No
c.56C>T	2		None	p.P19L	No
c.59C>A	2		None	p.A20E	No
c.60delG	2		None	p.A20fs	Yes
c.68C>T	2		None	p.S23F	No
c.104delAT	2		None	p.35fs	Yes
c.106delG	3		None	pV36fs	Yes
c.124T>C	3		None	pW42R	No
c.164C>A	3		None	p.T55K	No
c.166G>A	3		None	p.D56N	No
c.182-2A>G		3	Abolishment SA intron3	p.W61fs	Yes
c.183insCT	4		None	p.W61fs	Yes
c.198T>G	4		None	p.Y66X	Yes
c.193delT	4		None	p.Y65fs	Yes
c.222delC	4		None	p.W75fs	Yes
c.282delC	4		None	p.T95fs	Yes
c.303G>A		4	Abolishment SD intron 4	p.K101fs	Yes
c320T>C	5		None	p.L107P	No
c.345C>A	5		None	p.Y115X	Yes
c.417+1G>T		5	Abolishment SD intron 5	p.K139fs	Yes
c.419insG	6		None	p.G140fs	Yes
c.478delA	6		None	p.I159fs	Yes
c.507delC	6		None	p.P170fs	Yes
c.526delG	6		None	p.G176fs	Yes
c.537delCGGC	6		None	p.S179fs	Yes

Table : Mutations in REEP1 identified to date (Beetz et al., 2008, Slang et al., 2008).

To identify the molecular pathological mechanisms of the REEP1 mutations and the role of its different protein domains we examined the cellular expression pattern of the REEP1 carrying the mutations P19R and A20E. Both mutations affected residues that are part of the first transmembrane domain, predicted to be involved in protein localization (Beetz et al., 2010). The unpolar aminoacid (proline or alanine) are repleced with an aminoacid that has a R-basic group (arginine, in the case of REEP1[P19R]), or an

aminoacid that has a R-acid group (glutammic acid, in the case of REEP1[A20E]) modifying the hydrophobicity of the self-same domain. When expressed in Cos7 cells, both mutant proteins showed the same localization (data not shown).

Unlike the *wild-type*, the mutant protein was *present* in apparently empty inside *vesicles* that do not co-localize with the anti-PDI used to visualize ER (Figure). In order to characterize these vesicles and to investigate their possible origin, we first, carried out immunocytochemistry experiments. Using different antibodies to recognize the degradation protein pathways, we noticed, surprisingly, that none of these co-localized with vesicles. In Figure a is report, for instance, anti-ubiquitine utilized. It is an antibody against the homonymy protein involved in the first stage of the proteasomal patway activation. Upon different markers utilized to identify these vesicles only BODIPY 493/503 was able to co-localize with them (Figure b). BODIPY 493/503 contains a nonpolar structure that, upon binding to neutral lipid, emits a green fluorescence signal. BODIPY 493/503 is utilized to visualize lipid droplets (LDs) within cells. LDs are compartments found in most cell types that store neutral lipids such as triacylglycerol and cholesteryl ester. LDs are enriched in a variety of proteins known to be involved in lipid metabolism, membrane traffic and the structural integrity of the mono-phospholipid container (Tobias et al., 2008). To confirm our findings, Cos7 cells were transiently cotrasfected with an HA-tagged REEP[P19R] and a protein associated with LDs, ALDI-GFP (Associated with LD protein 1), carrying GFP sequence cDNAs. ALDI is a naturally occurring *bona fide* LD-resident protein, and. upon lipid loading of the cells, ALDI translocates from the ER into nascent LDs (Turrò et al., 2006). Confocal microscopy clearly showed that anti-HA and GFP signals co-localize perfectly, confirming that REEP[P19R] resides on the LDs (Figure c, d).

The use of three dimentional (3D) imaging software to confocal laser scanning microscopy (CLSM) allows us to visualize the spatial relationships between the objects within the cells. To evaluate better the relationship between REEP1 or REEP1[P19R] and LDs, Cos7 cells overexpressed the wild type or mutant proteins were immunostained with antibodies directed to REEP1 protein and BODIPY (493/503) and their detailed morphological behaviours were observed under a confocal laser microscope. For 3D reconstruction, series of optical sections were collected at 0.5-μm intervals along the Z-axis using the CLSM, and the immunocytochemical images were analyzed using a 3D

reconstruction software (Amira®, Visage Imaging Inc., Richmond, Au). As shown in Figure   REEP1^{WT} protein is close to LDs but not around them, whereas REEP1^{P19R} is totally around the LDs.

Finally, we used a biochemical approach to confirm our results. We used cell fractionation to verify the presence of REEP1^{P19R} to droplets. HepG2 cells were transfected with cDNA encoding mutant REEP1 and grown overnight in media supplemented with 200 μM oleic acid. The cells were harvested and separated into droplet (LD), cytosol (two different fraction cytosol 1 and cytosol 2) and total membrane (membrane) fractions. Equal amount of proteins of each fraction were separated by SDS-PAGE and processed by immunoblotting to detect markers for cytosol (α-actin), ER (calnexin) and droplets (caveolin). Immunoblots for caveolin, calnexin and actin confirmed that the fractions were well separated. REEP1^{P19R} was detected in both the droplet and membrane fractions (Figure). These results are in complete agreement with the immunofluorescence experiments.
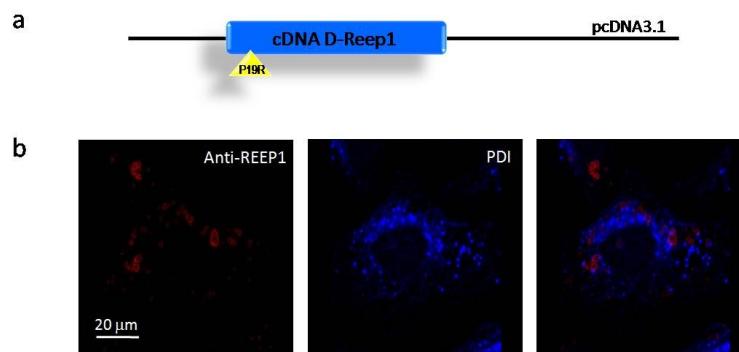
Figure : REEP1^{P19R} over-expression.
Cos7 cells expressing REEP1^{P19R} cDNA construct represents above (a), were costained with anti-REEP1 antibody to visualize REEP1^{P19R} protein (red) and anti-PDI antibody to visualize ER (b). The mutated protein forms vesicles and does not co-localize with ER. Scale bare: 20 μm.
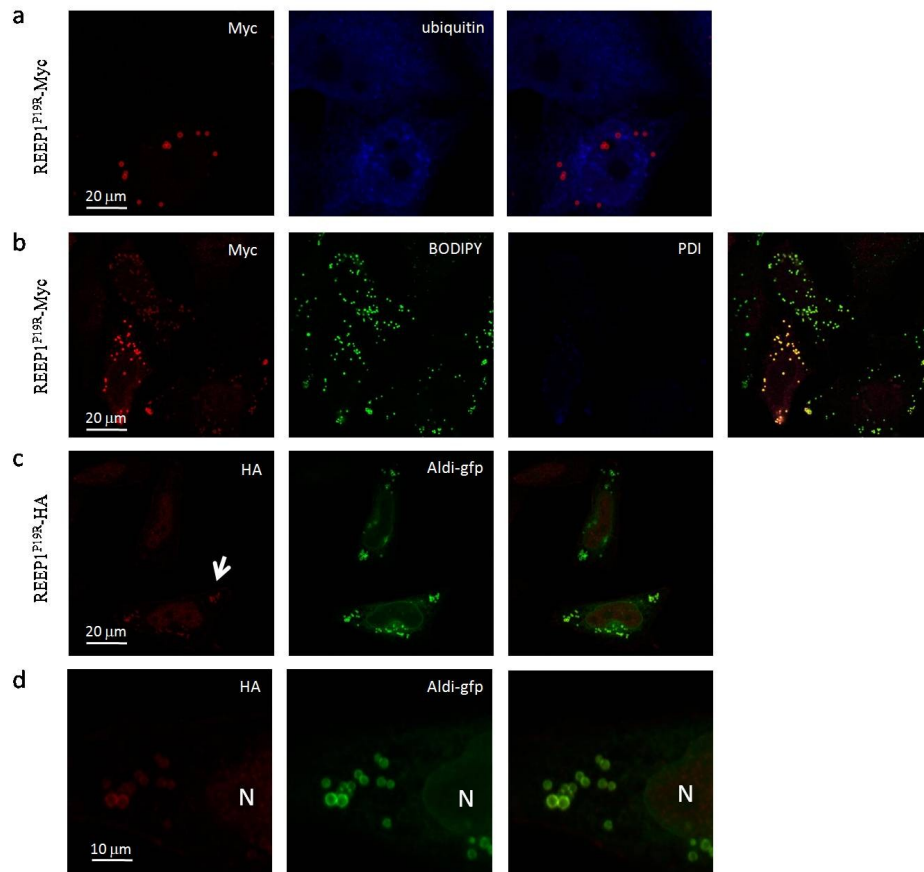
Figure : REEP1^P19R localization

Cos7 cells expressing Myc-tagged REEP1^P19R (red) were probed with (a) anti-ubiquitin antibody (Blue) or (b) anti-PDI antibody (blue) to visualize ER, and LDs marker BODIPY (493/503) (green). (c) Cos7 cells coexpressing HA-tagged REEP1^P19R (red) and a ALDI-GFP cDNA (green), a protein of the membrane of LDs. The d panels are higher magnification of the panels c). Scale bars: 20 μm (a, b, c) or 10 μm (d).
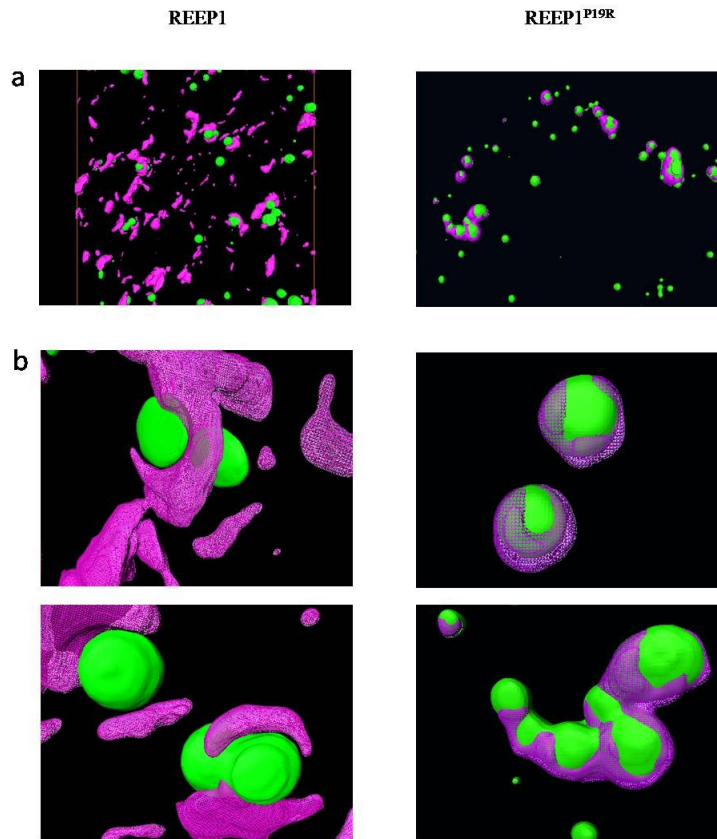
Figure : REEP1 and REEP1^{P19R} 3D reconstruction.
Three dimentional (3D) reconstruction of the LDs (green) and REEP1 proteins (wild type and mutated, violet) localization from a serial section of the Cos7 cells overexpressed REEP1 or REEP1^{P19R} (a). The series of optical sections were collected at 0.5-µm intervals along the Z-axis using the CLSM, and the immunocytochemical images were analyzed using 3D reconstruction software (Amira®, Visage Imaging Inc., Richmond, Au). The b panels are higher magnification of the panels a.
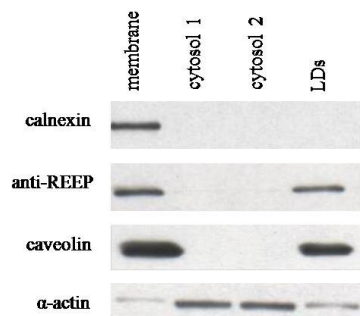
Figure : Cell fractionation shows that REEP^{P19R} is targeted to droplets.
HepG2 cells were trasfected with the REEP1^{P19R} cDNA construct. After cell fractionation, lipid droplets (LDs), total membrane (membrane) and cytosol (two different fractions cytosol 1 and cytosol 2) were separated by SDS-PAGE and then analyze by immunoblotting. Anti-REEP is used for visualize REEP1^{P19R} protein, anti-calnexin for the ER, anti-caveolin for the membranes and α-actin for cytosolic part.

3. REEP1 and REEP1[P19R] membrane topology

Integral membrane proteins as REEP1 represent an important class of proteins that are involved in a wide variety of cellular functions. Knowledge of the structure of proteins is crucial to understanding their function. Membrane topology software, available on the European Molecular Biology Laboratory (EMBL) protein prediction web site, was used to generate candidate membrane topology models for human REEP1 protein. The membrane topology predicted for REEP1 by the TM hidden Markov model (TMHMM) method (Krogh et al., 2001) used in these studies is shown in Figure . The software evaluates the hydrophobicity of the amino acid sequence and compares it with the hydrophobicity of polytopic proteins whose membrane topologies have been solved (Rost and Sander, 1993; Rost *et al.,* 1995, 1996). The REEP1 models predicted two putative and one hypothetical transmembrane domain (Figure a) with two possible orientation in the ER membrane: the first, with both the terminal parts face the cytoplasm (Figure b), and the second, with a C-terminal part that faces the cytoplasm while the N-terminal part that faces the luminal part of ER (Figure a). We know from literature that the C-terminal part of REEP1 protein faces the cytosol (Seong et al., 2010). We focalized our studies on the N-terminal part of the protein.

To investigate REEP1 membrane topology, two different experimental procedure were used: one based on immunofluorescence analysis and the second using a biochemical approach. In the first experiment, we monitored the REEP1 topology, by a selective permeabilization of cellular membranes. The assay is principally based on the ability of a gentle detergent to permeabilize only the cellular membrane, but not the organelles membrane; subsequently, a treatment with a protease is sufficient to cut specific bonds of the cellular proteins that look the cell cytoplasm (GFP is cutted off if it faces cytoplasm). So, after the protease treatment, it's possible to know if the GFP tag is oriented facing the cytosol or facing a protected luminal environment.

The orientation of the N-terminal part of REEP1 into the ER membrane was determined by GFP visualization in digitonin-permeabilized cells. Digitonin is a saponin that, in suitable conditions, can permeabilize only the cellular membrane, but not the membrane of the organelles The plasmatic membrane of digitonin-treated cells is selectively permeabilized while the ER membrane remains intact. To document this, HeLa cells were transiently transfected with REEP1-GFP (GFP is fused on N-terminal

part of the protein), treated with digitonin and immunostained with anti-PDI, an ER lumenal-specific marker and anti-GFP antibodies. Signal of GFP was observed in cells stained with the GFP antibody after Triton permeabilization (Methods Immunocytochemestry (ICC); Figure a) and digitonin treatment (Methods Selective membrane permeabilization; Figure b). An absence of signal was noted in cells treated with digitonin and stained with the ER luminal-specific PDI antibody, confirming the ER membrane was intact (Figure e), whereas signal was observed in the same cells, after subsequently treatment with Triton, stained with PDI-specific antibody (Figure f). After, cells expressing REEP1-GFP and permeabilized with digitonin, were exposed to trypsin, a proteolitic enzyme that cut selectively the Arg-Lys bonds (Figure c). The degradation of exposed GFP to cytoplasmic face after protease application is confimed by the lost of GFP signal. Finally, the organelles membrane is permeabilized by Tryton, but no signal is detected by anti-GFP (Figure d) and this definitively demonstrated that N-terminal part of REEP1 faces cell cytoplasm.

These data are confirmed by immunoisolation of membrane vesicles and membrane fractionation experiments. To determine the membrane orientation of the hydrophilic NH2-terminal and COOH-terminal ends of REEP1, we transiently transfected HeLa cells with HA-REEP1-Myc construct tagged at either its NH2-terminal with HA epitope and COOH- with Myc epitope. Cells expressing HA-REEP1-Myc were lisated, sonicated and centrifugated to obtain the membrane fraction (pellet) and the soluble fractions (supernatant). The pellet fraction was divided into three equal portions: the first portion was treated with proteinase K, an enzyme that has the ability to digest native proteins. In this way, if amino- or carboxy-terminal part of REEP1 faced the cytoplasm of the cell are digested and the specific antibody against HA or Myc tags are enable to recognize the cutted epitopes (Figure a). The remaining two portions were used one as a control for the fraction with proteinase K, and the other one is loaded directly on gel. Summarizing, finally we obtained five samples: the cell lysate after sonication (L), the supernatant (soluble fraction, S/N), pellet 1 (membrane fraction, P1), pellet called P2K (membrane fractions with digested protein by proteinase K), and pellet called P2 (membrane fraction control). Western blot analysis showed that HA and Myc are detectable in pellet fraction (P1), before the proteinase K treatment, and demonstrated that both, HA and Myc epitopes face the cell cytoplasm.

Based on data from experiments described below, we suggest a membrane topology for human REEP1 in which the hydrophilic NH2-terminal and COOH-terminal ends are proposed to extend into the cytosol while, the remaining portion, containing two membrane-spanning helices, embedded in the ER membrane. We repeat the experiment to investigate the topology of the missense pathological mutation REEP1^{P19R} (Figure b) to analyses if the aminoacid substitution can interferes with the right insertion of the protein in the lipid bilayer. Our result reveals that the mutated protein REEP1^{P19R} have the same topology of the wild type protein REEP1, with bot the extremities, N-terminal e C-terminal, faced the cytoplasm.

Figure : REEP1 membrane topology.
The informatic software predict two most probables topology for REEP1 protein. The first expected topology show that the C terminal part faces the cytoplasm of the cell instead N terminal part faces the luminal part of ER (a); the second one expected topology show that both the C and N terminal parts face the cytoplasm of the cell (b).
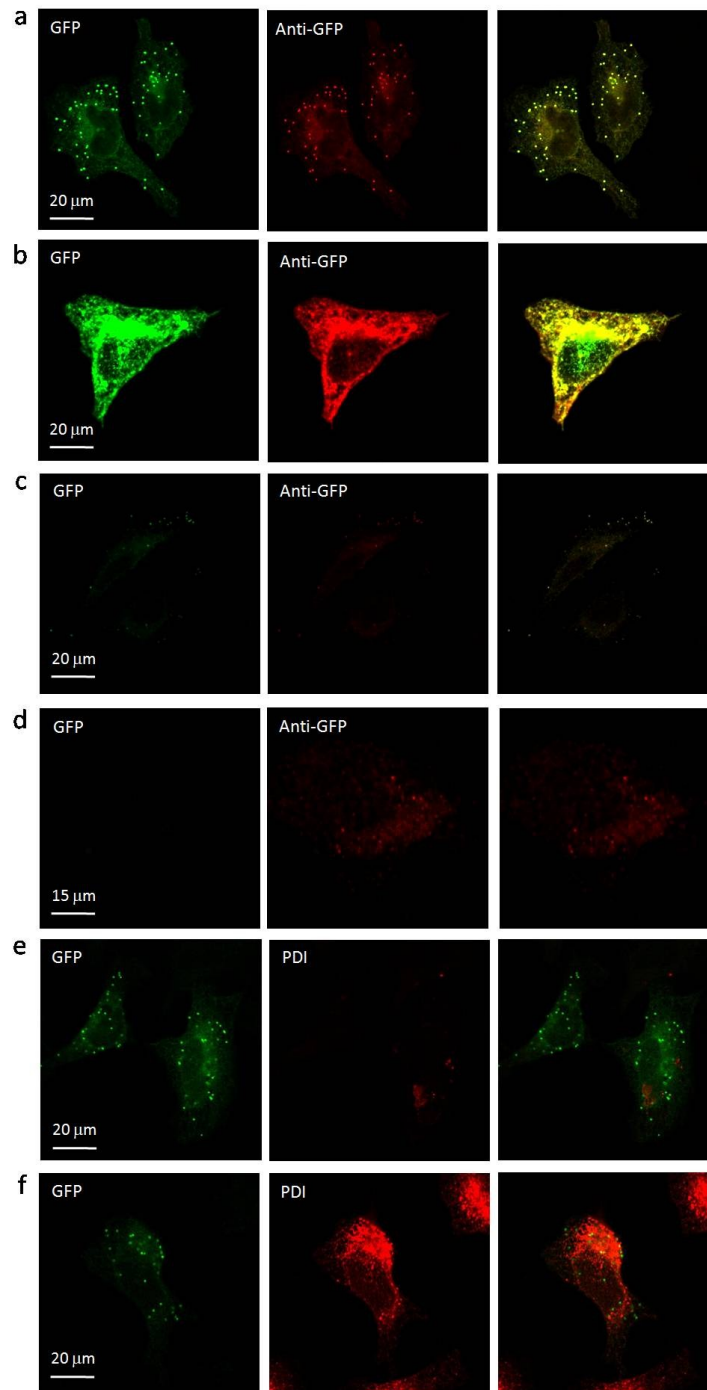
Figure : REEP1 N terminal part topology.
HeLa cells expressing GFP-REEP1. The immunocytochemistry show a normal staining with anti-GFP that recognize GFP-REEP1 (a). A second experiment consist in a selective permeabilization with digitonin , the GFP signal is detected by anti-GFP (b); after, the cells are treated with trypsin, a proteolitic enzyme (c) also in this case the GFP signal is detected by anti-GFP. Finally, the membrane of the organells are permeabilized by triton solution (d) and the GFP signal is detected by anti-GFP. PDI, an ER luminal protein, is used like a control that digitonin don't break the ER membrane during the selective permeabilization; (e) but anti-PDI recognise PDI protein after the triton treatment (f). Scale bars: 20 μm (a, b, c, e, f) or 15 μm (d).
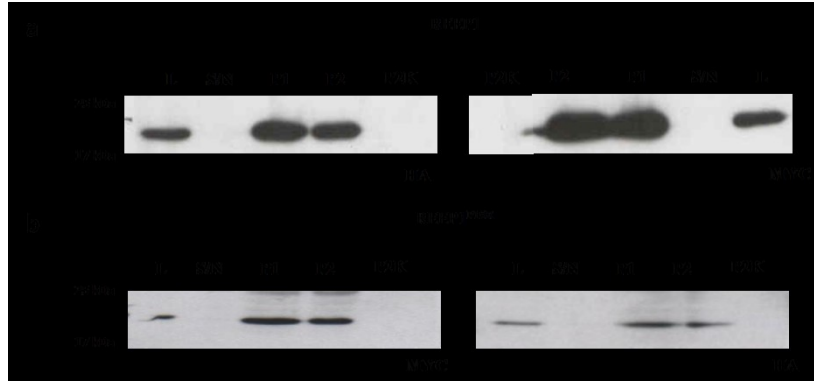
Figure : Topology of REEP1 and REEP1^{P19R} by immunoisolation of membranes .
HeLa cells were transfected with cDNA encoding N-terminally HA-tagged and C-terminally Myc-tagged REEP1. The cells are lisated (L), sonicated and, after centrifugation, the membranes fraction (pellet, P) were separated from the soluble fractions (supernatant, S/N). The pellet fraction is divided into three part: P1, P2 and a part in which proteinase K is added (P2K), an enzyme that has the ability to digest native proteins. The remaining two parts: one is a control for the fraction with proteinase K (P2), and the other one is loaded directly on gel (P1) (a). The same experiment was repeated transfecting the HeLa cells with with cDNA encoding N-terminally HA-tagged and C-terminally Myc-tagged REEP1^{P19R} (b).

4. REEP1 form vesicles around LDs in appropriate conditions

LDs are compartments found in most cell types that store neutral lipids; because of its droplet morphology, this compartment has long been considered to be an inert container devoid of metabolic activity. Recent proteomic studies have found that LDs are enriched in a variety of proteins known to be involved in lipid metabolism, membrane traffic and the structural integrity of the mono-phospholipid container (Athenstaedt et al., 1999; Brasaemle et al., 2004; Fujimoto et al., 2004; Liu et al., 2004; Murphy, 2001). Moreover, detailed lipidomic studies attest to the complexity and specialization of the lipid composition of this compartment (Bartz et al., 2007a; Murphy 2001; Tauchi-Sato et al., 2002).

At this point of our studies, we wondered if wild type REEP1 actually doesn't localized around the vesicles because it performs its function in another place or REEP1, indeed, in some way to go around the LDs, but it's degraded immediately and we can't see it.

4.1. Inhibition of proteasomal pathway or autophagy

ApoB is the primary structural protein of VLDL. It is synthesized on membrane-bound ribosomes and translocated to the ER lumen cotranslationally. Nascent lipoprotein particles are first assembled in the rough ER, and after maturation in the smooth ER and possibly in the Golgi, they are secreted by exocytosis (Davis, 1999). When conditions are not appropriate for VLDL assembly, ubiquitination and proteasomal degradation of ApoB increase. In contrast to most other proteins that probably undergo retrotranslocation from the ER lumen for ER-associated degradation, ApoB is thought to remain halfway through the translocon before being extracted to the cytoplasm for degradation (Fisher and Ginsberg, 2002); thus, proteasomes where ApoB is degraded are likely to be in the proximity of the ER. Subsequent experiments revealed that the ApoB accumulation around LDs increased markedly when either proteasomal function or autophagic pathway were inhibited. Ubiquitinated ApoB, proteasomal subunits, and autophagic vacuoles were all found in or around the ApoB-positive LDs. The observation indicates that LDs provide a site to hold amphipathic ApoB without gross aggregation, where proteasomal and autophagic pathways converge for degradation (Ohsaky et al., 2006). To investigate if REEP1 expression is regulated

through the degradative proteosome and autophagic pathways we reproduced the same experiments on REEP1 transfecting cells.

Cos7 cells were transiently transfected with REEP1 cDNA with fused the Myc epitope, and treated; with 200μM oleic and linoleic acids to increase the lipids pathway. and three hours before cells fixation, cells were incubated in medium containing 10μM *N*-acetyl-l-leucinyl-l-leucinyl-l-norleucinal (ALLN; Sigma-Aldrich) to inhibit proteasome functions, or 10 μM 3-methyladenine (3-MA; Sigma-Aldrich) to inhibit autophagy.

Surprisingly, in accordance with ApoB results described above, also REEP1 localization is different in appropriate conditions, and, in particularly it's evident that increasing fatty acids pathway and inhibiting the autophagy (Figure), or the proteasomal pathway (Figure) REEP1 is localized around LDs.

These data suggest that REEP1 may be involved in LDs vesicles biogenesis; in accordance with the DP1/Yop1p family ability to remodel the membrane gives to the two transmembrane domains. REEP1, in fact, is localized into the ER membrane and it could be involved in the curvature of ER membrane to form a LDs vesicles and make sure that the vesicles have the right curvature to close themselves and leave the ER to transport their contempt where is necessary.
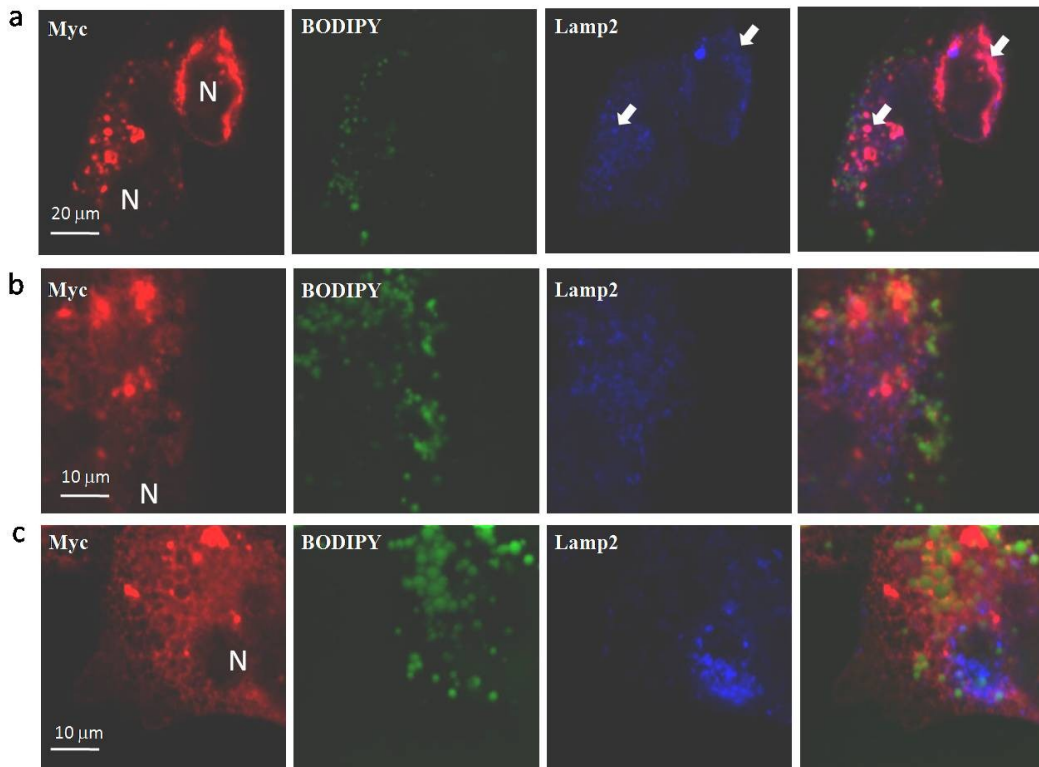
Figure : Inhibition of autophagy.

Cos7 cells expressing REEP1 cDNA with Myc epitope fused at C-terminal part were costained with anti-Myc (red) to visualize REEP1 protein, LDs marker BODIPY 493/503 (green) and anti-LAMP2 antibody (blue) to visualize autophagosomal-lysosomal compartment, without any treatment (a). Arrows highlight the colocalization of the REEP1 and LAMP2 signals suggesting that REEP1 could be degraded by autophagosomal-lysosomal pathway. The cells were cultured in the presence of supplemental oleic and linoleic acid to improve the fatty acid patway (b); in this condition the lipid number increases, note that REEP1 expression seems change and a little amount of protein localizes around the LDs. Then, the cells were cotreated with 3-methyladenine (3-MA), an inhibitor of endogenous protein degradation and appears to act specifically upon the autophagic/lysosomal pathway of degradation (c); note that REEP1 protein localizes around LDs when the *lipid* content is increase and degradation autophagic/lysosomal pathway is inhibited. N= nucleus. Scale bars: 20 µm (a) or 10 µm (b, c).
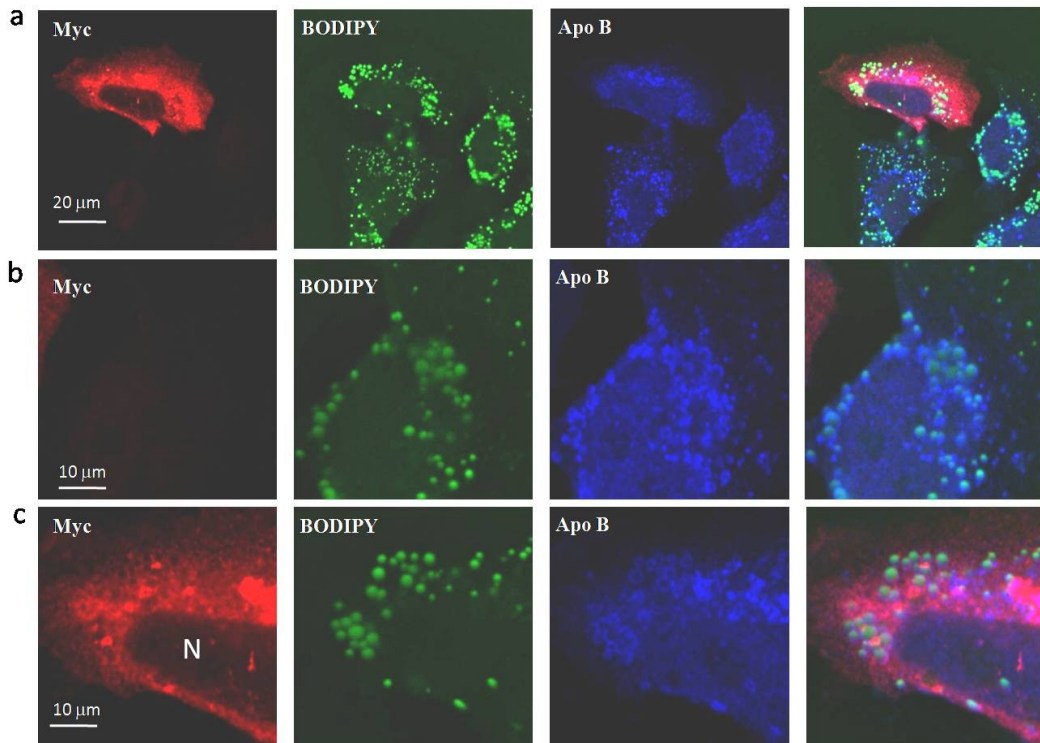
Figure : Inhibition of proteasomal pathway.
Cos7 cells expressing REEP1 cDNA with Myc epitope fused at C-terminal were cultured in presence of supplemental oleic and linoleic acid to improve the fatty acid content and cotreated with N-acetyl-leu-leu-norleucinal (ALLN), an inhibitor of the ubiquitin-proteasome pathway. The cells were costained with anti-Myc (red) to visualize REEP1 protein, LDs marker BODIPY (493/503) (green) and apolipoprotein B-100 (Apo B) antibody (blue), a protein found adjacent to LDs and that is degradated by proteasomal pathway (a). In (b) there is an magnification of a non trasfected cell, in (c) there is an magnification of a transfected cell. Scale bars: 20 μm (a) or 10 μm (b, c).

4.2. REEP1 returns to ER when droplets regress

There are several models to explain droplets biogenesis but nothing is known about how droplets regress. There is some proteins behave as integral membrane proteins that are inserted into the ER, transferred from their site of insertion to droplets independently of COPII vesicles and return to the ER when droplets are induced to regress. These findings suggest that droplets directly form from and return to the ER as part of a cyclic process of neutral lipid expansion and retraction (Zehmer et al., 2009). We want demonstrate that REEP1 behaves like these proteins if we increase the fatty acids pathway adding into the medium oleic and linoleic acid and block the proteic synthesis by using cycloheximide.

Thus, Cos7 cells were transfected with the cDNA of REEP1 by using *TransIT®-LT1* Transfection Reagent (Mirus) and grow them for 8 hours; immunofluorescence using anti-REEP had an ER staining pattern that matched that observed with anti-PDI and REEP1 protein don't localizes around LDs (Figure a). The LDs are visible, as judged by staining with the fluorescent neutral lipid dye BODIPY 493/503 dye. By contrast, when cells are grown under the same conditions followed by 15 hours in presence of both 100μM of a mix of oleic and linoleic acid and 50μg/ml cycloheximide, the majority of anti-REEP1 staining was on the surface of BODIPY 493/503 dye positive LDs (Figure b).

We demonstrated that increasing the lipid metabolism of cells REEP1 localizes around LDs. These result suggest that REEP1 is directly involved in LDs biogenesis and its localization depends of the energetic cell status. The experiment is repeated for REEP1[P19R] protein and, like REEP1, the majority of anti-REEP1 staining was on the surface of BODIPY 493/503 dye positive LDs (data not shown).

Just as droplets form under conditions of fatty acid excess, they regress when cells are deprived of fatty acids. Little is known about the fate of droplet proteins when LDs disappear from the cell. Both ADRP (Masuda et al., 2006; Xu et al., 2005) and perilipin (Xu et al., 2006) are degraded by the ubiquitin-proteasome pathway when triacylglycerol recycling is disrupted by the long chain acyl-CoA synthetase inhibitor triacsin C. We used triacsin C to reduce LDs in the cell and followed the fate of transfected REEP1-GFP constructs.
only come from regressing LDs.

We used immunofluorescence to identify the destination of REEP1 when droplets disappear from the cell. We transfected Cos7 cells with a cDNA encoding REEP-GFP and REEP1^{P19R}-GFP and grew them for 3 hours before adding oleic acid to induce LDs. Cells were incubate an additional 6 hours and either fixed or incubate in presence BSA, 7.5µM triacsin C and cycloheximide for 15 hours before processing for immunofluorescence. REEP1 and REEP1^{P19R} localized to LDs in cells with droplets (Figure a, c). Cells treated with triacsin C, by contrast, lost all their droplets (BODIPY 493/503) and both REEP1 and REEP1^{P19R} were exclusively reticular (Figure b, d). In the absence of protein synthesis, the REEP1 and REEP1^{P19R} in the ER could have only come from regressing LDs.
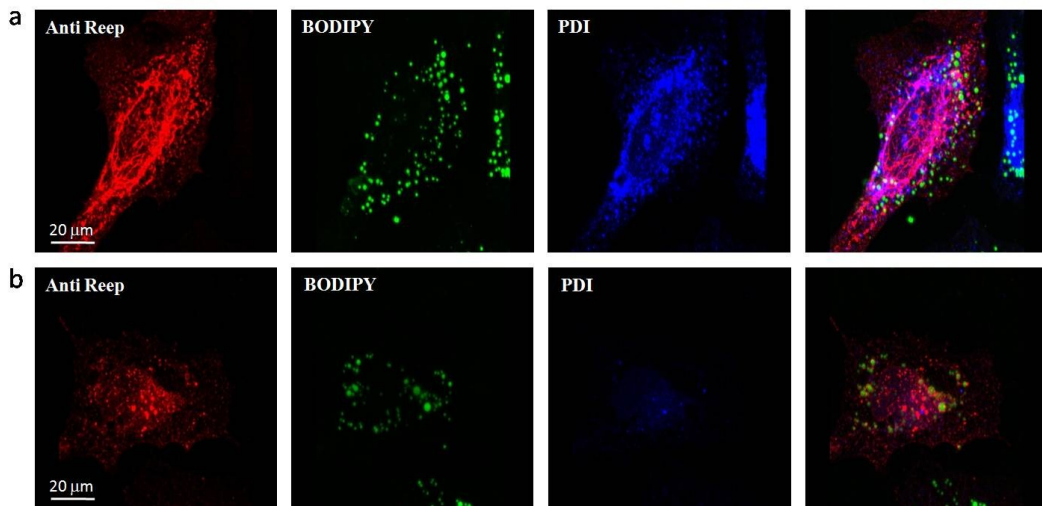
Figure : Inhibition of proteic synthesis.
Cos7 cells are transfected with the REEP1 cDNA. The cells were costained with anti-REEP1 (red), LDs marker BODIPY 493/503 (green) and anti-PDI antibody (blue) to visualize ER. The culture medium is supplementated only with oleic and linoleic acid (a). Then, the cells were cotreated with cycloheximide, an inhibitor of protein biosynthesis (b). Scale bar: 20 µm (a, b).
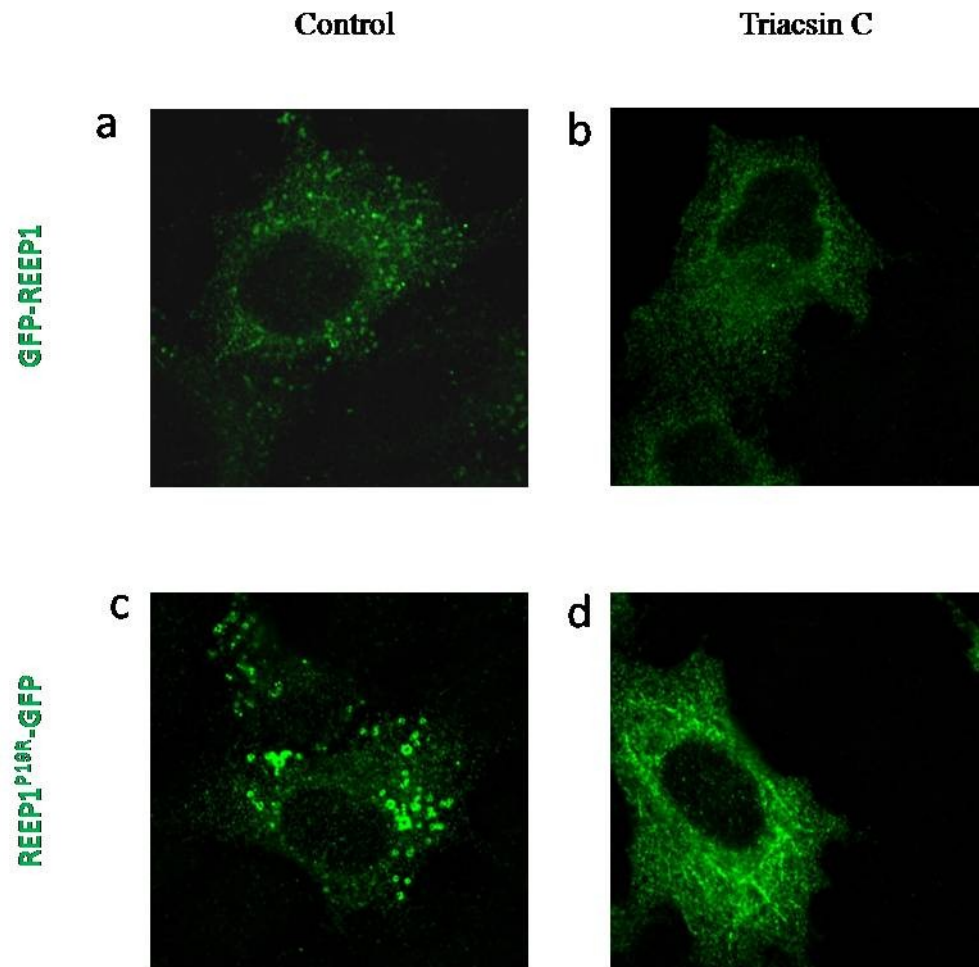
Control **Triacsin C**

a
b
c
d

GFP-REEP1

REEP1^{P19R}-GFP

Figure : REEP1 on LDs return to the ER upon droplet regression.
(a, b) Cos7cells on coverslips were transfected with GFP-tagged REEP1. Three hours after transfection, oleate was added and the cells incubated for an additional 6 hours. Cells were then either fixed (a) or incubated in thepresence of 1 mg/ml BSA, 50 µg cycloheximide and 7.5 µg/ml triacsin C for 3 hours (b) before processing the samples forimmunofluorescence. In thecontrol cells the majority of REEP1 was vesicular (b). In triacsin-C-treated cells, very few or no vesicles were detected and REEP1 was found in a reticular pattern (b). (c, d) Cos7 cells on coverslips were treated as in a and b, except they were transfected with GFP-tagged REEP1^{P19R}. Scale bar: 20 µm (a, b, c, d).

5. REEP1 is able to homo-oligomerization while REEP1^{P19R} do not

Members of the DP1/Yop1p protein family form higher-order oligomeric structure (Shibata et al., 2008). Since REEP1 is structurally similar to the DP1/Yop1p proteins we made Co-Immunoprecipitaion assay (Co-IP) to verify the REEP1 and REEP1^{P19R} ability to homo-oligomerization. Co-IP is a common technique used for protein interaction discovery. An antibody for the protein of interest, linked to a support matrix, is incubated with a cell extract so that the antibody will bind the protein in solution. The antibody/antigen complex will then be pulled out of the sample (precipitation): this physically isolates, from the rest of the sample, the protein of interest and other proteins potentially bound to it (co-immunoprecipitation). Finally, components of the immuno complex (antibody, antigen and co-immunprecipitated proteins) are analyzed by SDS-PAGE and Western blot.

To test if REEP1 has the ability to form homo-oligomers, Cos7 cells were co-transfected with REEP1-HA and REEP1-Myc expression constructs. Lysates prepared from these cells were immunoprecipitated using anti-Myc antibodies. The immunoprecipitate was analyzed by western blotting with both anti-Myc and anti-HA antibodies. The presence of both Myc and HA signals in the immunoprecipitate showed that immunoprecipitation of REEP1-Myc pulled down also REEP1-HA thus demonstrating that REEP1 molecules are capable of self-association (Figure a).
We repeated this experiment for the missense mutation REEP1^{P19R}. Surprisingly, the mutated form of REEP1 protein was not capable to homo-oligomerize (Figure b).

These results allow us to find a first significant sign of a different interaction between the *wild type* and the mutated proteins; so, we supposed that the aminoacid replacement in nineteen position prevents the self-association of REEP1^{P19R}, so we could conclude that this part of the protein is an important site of self-association; the homo-oligomerization appears fundamental the function of the protein, and this could be the cause of the pathogenicity of this mutation.
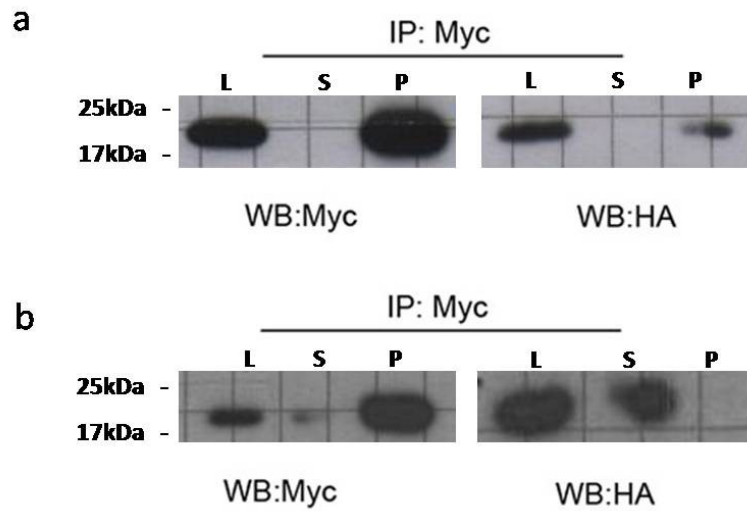
a

IP: Myc

| | L | S | P | | L | S | P |

25kDa –
17kDa –

WB:Myc   WB:HA

b

IP: Myc

| | L | S | P | | L | S | P |

25kDa –
17kDa –

WB:Myc   WB:HA

Figure : REEP1 is capable of homo-oligomerization.
Cos7 cells were co-transfected with REEP1-Myc and REEP1-HA constructs. Lysate prepared from these cells are immunoprecipitated using anti-Myc antibodies. Immunoprecipitates were analyzed by western blot with both anti-HA and anti-Myc antibodies. The ability of anti-Myc to immunoprecipitate REEP1-HA demonstrates that REEP1 forms oligomers (a). On the contrary, Cos7 cells are co-transfected with REEP1-Myc and REEP1^{P19R}-HA constructs. The experiment was repeated and immunoprecipitates were analyzed by western blot with both anti-HA and anti-Myc antibodies. The inability of anti-Myc to immunoprecipitate REEP1-HA demonstrates that REEP1^{P19R} do not forms oligomers (b).

6. REEP1^{A132V} localization

The collaboration with Prof. Mostacciuolo lab at the department of Biology of University of Padua, lead us to start analyze a novel pathological missense mutation of REEP1: REEP1^{A132V} . This mutation has not yet been published and is characterized by the substitution of the basic amino acid arginine, with the polar amino acid valine.

This mutation is situated in the C-terminal part of REEP1, in a region that appear involved in the interaction with microtubules. To determine the endogenous REEP1^{A132V} protein expression pattern and define exactly its subcellular localization, we generated tagged-Myc and untagged REEP1^{A132V} constructs. We transiently transfected Cos7 cells with untagged REEP1^{A132V} and REEP1^{A132V}-Myc cDNAs . Cell expressing REEP1^{A132V} were fixed and stained with antibosies to visualize REEP1, the epitope Myc, the ER and microtubules. From immunostaining experiments and confocal analysis of transfected cells we observed that REEP1^{A132V} localized with ER structure (Figure a) and partially overlapped the microtubules cytoskeleton (Figure Figure   b). The REEP1^{A132V} expression suggeste a defective interaction between REEP1, ER and microtubules. More analysis are needed to comprehend the functional modification produced in REEP1 by the aminoacidic substitution in position 132.
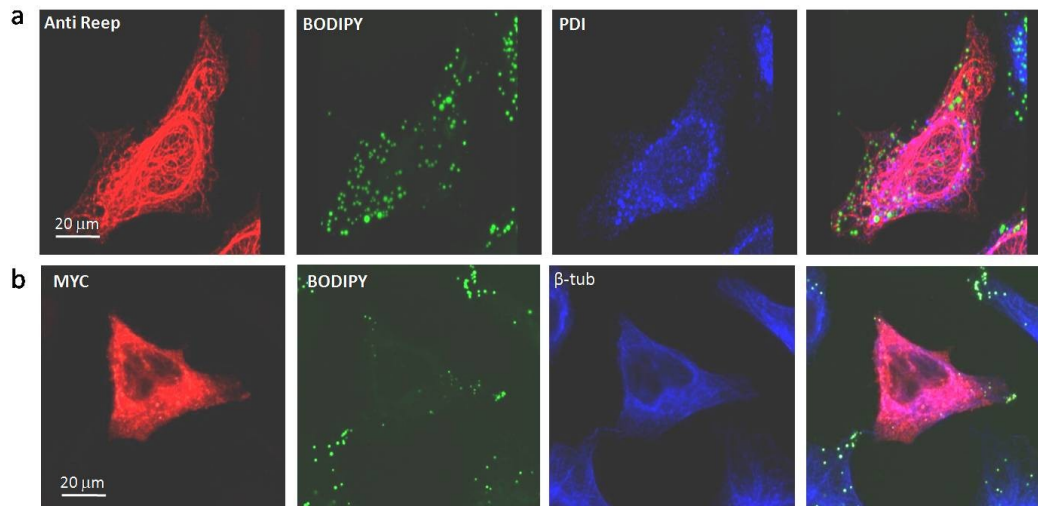
Figure : REEP1^{A132V} localization.

Cos7 cells are trasfected with the construct that contain REEP1^{A132V} cDNA (a). Anti-Reep antibody is used to visualize REEP1^{A132V} protein (red). Cells were costained with anti-PDI antibody (blue), LDs marker BODIPY (493/503) (green). The pictures show that the mutated protein is reticolar and partially co-localize with ER. Cos7 cells were trasfected with the construct that contain REEP1^{A132V} cDNA with fused Myc epitope in the C-terminal part (b). Cells were costained with anti-β-tubulin antibody (blue), LDs marker BODIPY (493/503) (green). The panels shows that the mutated protein partially co-localize even with microtubules. Scale bar: 20 μm (a, b).

12.   DISCUSSION

Mutations of the *SPG31* gene, which encodes for REEP1protein, are responsible for a dominant form of Hereditary Spastic Paraplegia (HSP); HSPs are a clinically and genetically group of inherited disorders mainly characterized by progressive lower extremity spasticity and weakness.

REEP1 is a member of the DP1/Yop1p family; this family has the characteristic of forming oligomers as for example reticulons and DP1/Yop1p proteins form oligomers that are relatively immobile in the membrane. The oligomerization of the reticulons and DP1/Yop1p plays an important role in the proper localization of these proteins in the ER and for tubule formation in living cells (Shibata et al., 2008). Our data suggest that this process is fundamental for the correct functionality of REEP1; we demonstrate *in vitro* that the wild type protein is capable to oligomerize, while the pathological mutation REEP1^{P19R}, that present an aminoacidic substitution in the first transmembrane domain not. This result is important from a functional point of view: it's evident that the mutated form of the protein fails to perform its normal function. Moreover the mutated protein presents significant differences compared to REEP1wild type: REEP1^{P19R} changes its localizations switching from ER to LDs and its expressions going from reticular distribution of REEP1 perfectly overlapped on ER to a vesicular form in REEP1^{P19R} that we have demonstrate surround LDs. So, REEP1^{P19R} incapacity to perform its correct function given by the inability to dimerize associated with the difference of expression and localization, at this time of study, are the only proven causes that explains the difference between the wild type protein and the pathological mutation.

Another pathological mutations, REEP1^{A132V}, that we started study thank to the collaboration with Prof.ssa Mostacciuolo laboratory, has demonstrated a different localization respect to wild type protein. We know that C-terminal tail of REEP1 is both necessary and sufficient for interaction with microtubules (Seong et al., 2010) and our preliminary studies reveal that this mutation is equally distributed from ER and microtubules. So, even in this case, the pathological mutation has a different localization respect the wild type protein which results in pathogenicity and,

consequently leads to the onset of HSPs. However, other studies are needed for characterize this mutation.

An unexpected but fundamental result is that REEP1, in appropriate conditions, is localized around LDs. In fact, we have shown that increasing the fatty acids pathways adding oleic and linoleic acids into the culture medium, the wild type protein is seen in correspondence of the LDs membranes forming vesicles around these structures. This finding isn't a REEP1peculiarity because also DGAT2, the major enzyme catalyzing TG synthesis, localizes primarily to the ER but, when the cells are treated with oleic and linoleic acid, relolizes to LDs surface (Kuerschner et al., 2008).

This discovery open a new research field. While the first part of our studies is focalized on the relationship between the protein and the ER because our data suggested that REEP1 was an ER protein, in the second experimental part our attention is shifted on the relationship between ER and LDs. In eukaryotes, evidence suggests that LDs are often tightly associated and sometimes appear to be connected with the ER. In some instance, sheets of ER membrane even partially surround the droplet, cradling it like an eggcup (Robenek et al., 2006). In addition, the enzymes (Buhman et al., 2001) that catalyze the synthesis of neutral lipids in the droplet core are localized predominantly to the ER. In fact, the enzyme DGAT2 (Lardizabal et al., 2001; Cases et al., 2001), localizes to areas where droplets are tightly associated with ER under conditions that promote droplet formation (Kuerschner et al., 2008).

It's interesting to note that LDs have a unique structure with an organic lipid phase surrounded by a single layer of polar lipids, that makes it difficult to comprehend the relations between LDs and the associated proteins. The normal conformation of transmembrane proteins, with water-soluble domains on both sides of a membrane bilayer, should not allow targeting of these proteins to the monolayer droplet surface (Ostermeyer et al., 2001). However, it's possible that REEP1 laterally flows from ER to LDs, if we suppose that REEP1 have the same topology of REEP5-6/Yop1p with the hairpin domain inserted only into the external layer of the ER phospholipidic bilayer; this is most likely because our result on topology studies reveals that both C-terminal and N-terminal domains of the protein face the cell cytoplasm and the transmembrane domain are not so long to inserted completely into the phospholipidic bilayer. So, further studies are needed to determin the exact topology of the hairpin domains.

At this point, we are focalized on the probable function of REEP1 in LDs biogenesis. The droplets remain tethered to the ER, and the monolayer surrounding them is continuous with the ER bilayer; lipids could diffuse laterally into the droplet. However, if lipid droplets accumulate neutral lipids after detaching from the ER, these lipids must either be synthesized at the droplet surface or be transferred to droplets by a dedicated mechanism that might involve specific transfer proteins, analogous to ceramide transfer proteins, glycerolipid transfer proteins, or oxysterol binding proteins (Levine et al., 2006; Schulz et al., 2007; Hanada et al., 2007; Brown and Mattjus, 2007).

How lipids are transferred from the site of synthesis to LDs is unknown. We demonstrate that REEP1 shifts from the ER and appears around LDs when the fatty acids pathway is increased and when the protein biosynthesis is inhibited by cycloheximide, an inhibitor of protein biosynthesis in eukaryotic organisms; it's evident that in particularly conditions of fatty acids abundance or proteins lack, REEP1 is located exactly where it exerts its function, in LDs monolayer membrane. Exactly, what is REEP1 function is not known but our hypothesis expected that REEP1 is involved not only in biogenesis of LDs, but even in the energy balance of the cell. The balance of lipids stored within LDs is controlled by the net cycle of neutral lipid synthesis and degradation. Neutral lipids in the core of the droplet are hydrolyzed by intracellular lipases (Zechner et al., 2005), yielding fatty acids for energy generation and anabolism of membrane phospholipids. The liberated fatty acids may be oxidized in mitochondria in mammalian cells or in peroxisomes in yeast (Binns et al., 2006) to generate ATP. Cycles of esterification and lipolysis are likely to be continuously active in smaller droplets of most cells. The PAT proteins on smaller droplets may afford some protection from lipolysis (Sztalryd et al., 2006), but basal levels of lipolysis are usually detectable. On the other hand, droplets in adipose tissue or in the fat bodies of flies are major energy reserves for the organism. Therefore, the storage and utilization of lipids likely involve more complex regulation. We found that REEP1 return to the ER where it appear largely to be preserved. This suggest that the phospholipid monolayer surrounding each LDs returns to the ER when neutral lipid is depleted by triacsin C. The return of REEP1 to the ER is essentially the reciprocal of REEP1 movement to existing droplets. If LDs are always attached to the ER through a thin stalk then REEP1 can easily return through the stalk. The stalk, in other words, functions as a conduit through

which droplet and REEP1 can travel to and from the ER, according to the energy balance of the cell. It's interesting to note that also REEP1^{P19R} behaves like REEP1: when the neutral lipid is depleted by triacsin C, the protein return to ER, and, for the first time, it lost the typical vesicular feature to take a fragmented appearance, supporting our theory on the involvement of REEP1 in the energetic cell status.

In this moment the physiophathological mechanism that explain why the disease involves specifically the longer neurons of the spinal cord is unknown .The most accredited hypothesis is that this protein disfunctions involved in HSP lead disaggregation of the axonal transport of macromolecules, organels and other substances, and predominantly affect the distal part of these neurons (Crosby et al., 2002; Soderblom et al., 2006). The largest number of known HSP genes encodes proteins implicated with varying degree of certainty into the general class of trafficking and transport proteins (Soderblom and Blackstone, 2006). Considering our results, in accordance to the literature, we can propose a new hypothesis for spg31 linked HSP in which REEP1 defects can modify the equilibrium of LDs formation or transport pathway. It's possible that a defect in LDs transport could impaired not only the functionality of motoneurons but also the vitality of the same neuron. We want to remember that this type of neurons can reach lengths to 1.5 meters and a defect in this vesicular traffic prevents that the nutritive substances, receptor, and all other substances that are contained in LDs arrive where they need to get, with a dramatic evolution for the cell survival.

13.   REFERENCES

Allan V.J. and **Vale** R.D. (1991). "Cell cycle control of microtubule-based membrane transport and tubule formation in vitro." *J. Cell Biol.*, **113**: 346-359.

Athenstaedt K. et al. (1999). "Identification and characterization of major lipid particle proteins of the yeast saccharomyces cerevisiae." *J. Bacteriol.* **181**: 6441-6448.

Barnea et al. (2004). "Odorant receptors on axon termini in the brain." *Science.* **304** (5676):1468.

Bartz R. et al. (2007a). "Lipidomics reveals that adiposomes store ether lipids and mediate phospholipid traffic." *J. Lipid Res*. **48**: 837-847.

Beetz C. et al. (2010). "Mutational spectrum of the SPG4 (SPAST) and SPG3A (ATL1) genes in Spanish patients with hereditary spastic paraplegia." *BMC Neurol.* **8**:10:89.

Beetz C. et al. (2008). "REEP1 mutation spectrum and genotype/phenotype correlation in hereditary spastic paraplegia type 31" *Brain* **131**(Pt 4):1078-1086.

Behan W.M. and **Maia** M. (1974). "Strumpell's familial spastic paraplegia: genetics and neuropathology." *J. Neurol Neurosurg Psychiatry* **37**(1): 8-20.

Behrens M. et al. (2006) "Members of RTP and REEP gene families influence functional bitter taste receptor expression." *J. Biol Chem.*; **281**(29): 20650-20659.

Binns D. et al. (2006). "An intimate collaboration between peroxisomes and lipid bodies." *J Cell Biol.* **173**:719-731.

Blackstone C. et al. (2011). "Hereditary spastic paraplegias: membrane traffic and the motor pathway." *Nat Rev Neurosci.* **12**(1): 31-42. **Review**. Erratum in: Nat Rev Neurosci. **2011** Feb;12(2):118.

Boström P. et al. (2007). "SNARE proteins mediate fusion between cytosolic lipid droplets and are implicated in insulin sensitivity." *Nat Cell Biol*. **9**: 1286-1293.

Brady A.E. and **Limbird** L.E. (2002). "G protein-coupled receptor interacting proteins: emerging roles in localization and signal transduction." *Cell Signal*. **14**(4): 297-309.

Brasaemle D.L. et al. *(*2004*). "*Proteomic analysis of proteins associated with lipid droplets of basal and lipolytically stimulated 3T3-L1 adipocytes.*" J. Biol Chem.* **279***: 46835-46842.

Brasaemle D.L. (2007). "The perilipin family of structural lipid droplet proteins: stabilization of lipid droplets and control of lipolysis." *J. Lipid Res.* **48**: 2547-2559.

Brown D.A. (2001). "Accumulation of caveolin in the endoplasmic reticulum redirects the protein to lipid storage droplets." *J. Cell Biol*. **152**: 1071-1078.

Brown R. and **Mattjus** P. (2007) "Glycolipid transfer proteins." *Biochim Biophys Acta.* **1771**: 746–760.

Brown M.S. et al. (1980). "The cholesteryl ester cycle in macrophage foam cells: continual hydrolysis and re-esterification of cytoplasmic cholesteryl esters." *J. Biol Chem.* **255**: 9344-9352.

Buhman K.K. et al. (2001). "The enzymes of neutral lipid synthesis." *J. Biol Chem.* **276**: 40369-40372.

Cacchiaro J.L. et al. (2008). "Cytoplasmic lipid droplets are translocated into the lumen of the Chlamydia trachomatis parasitophorous vacuole." *Proc Natl Acad Sci* USA **105**: 9379-9384.

Cases S. et al. (2001). "Cloning of DGAT2, a second mammalian diacylglycerol acyltransferase, and related family members." *J. Biol Chem.* **276**: 38870-38876;

Chen C.N. et al. (2002). "AtHVA22 gene family in Arabidopsis: phy-logenetic relationship, ABA and stress regulation, and tissue-specific expression." *Plant Mol Biol.* **49**(6): 633-644.

Connell J.W. et al. (2009). "Spastin couplet microtubule severing to membrane traffic in completion of cytokinesis and secretion." *Traffic.* **10**(1): 42-56.

Crosby A.H. and **Proukakis** C. (2002). "Is the transportation highway the right road for hereditary spastic paraplegia?" *Am J Hum. Genet.* **71**: 1009-1016.

Davis R.A. (1999). "Cell and molecular biology of the assembly and secretion of apolipoprotein B-containing lipoproteins by the liver." *Biochim Biophys Acta* **1440**: 1–31.

Dayel M.J. and **Verkman** A.S. (1999). "Diffusion of green fluorescent protein in the aqueous-phase lumen of the endoplasmic reticulum." *Biophys J.*, **76**: 2843-2851.

Depienne C. et al. (2007). "Hereditary spastic paraplegias: an update." *Curr Opin Neurol* **20**(6): 674-680.

Dreier L. and **Rapoport** T.A. (2000). "*In vitro* formation of the endoplasmic reticulum occurs independently of microtubules by a controlled fusion reaction." *J. Cell Biol.*, **148**: 883-898.

Dube M.P. et al. (1997). "Hereditary spastic paraplegia: LOD-score considerations for confirmation of linkage in a heterogeneous trait." *Am J Hum Genet* **60**(3): 625-629.

Ducharme N. and **Bickel** P. (2008). "Lipid droplets in lipogenesis and lipolysis." *Endocrinology* **149**: 942-949.

Ebbing B. et al. (2008). "Effect of spastic paraplegia mutations in KIF5A kinesin on transport activity." *Hum Mol Genet.* **17**: 1245-1252.

Ehehalt R. et al. (2006). "Translocation of long chain fatty acids across the plasma membrane-lipid rafts and fatty acid transport proteins." *Mol. Cell Biochem.* **284**: 135-140.

Errico A. et al. (2002). "Spastin, the protein mutated in autosomal dominant hereditary spastic paraplegia, is involved in microtubule dynamics." *Hum Mol Genet* **11**(2): 153-163.

Evans K. et al. (2006). "Interaction of two hereditary spastic paraplegia gene products, spastin and atlastin, suggests a common pathway for axonal maintenance." *Proc Natl Acad Sci U S A* **103**(28): 10666-10671.

Fei W. et al. (2008). "Fld1p, a functional homologue of human seipin, regulates the size of lipid droplets in yeast." *J. Cell Biol.* **180**: 473-482.

Fink J.K. (2003). "Advances in the hereditary spastic paraplegias." *Exp Neurol* **184 Suppl 1**: S106-10.

Fisher E.A. and **Ginsberg** H.N. *(*2002*). "*Complexity in the secretory pathway: the assembly and secretion of apolipoprotein B-containing lipoproteins.*" J. Biol Chem.* **277***: 17377-17380.*

Fujimoto Y. et al. (2004) "Identification of major proteins in the lipid droplet-enriched fraction isolated from the human hepatocyte cell line HuH7." *Biochim Biophys Acta* **1644**: 47-59.

Fujimoto T. et al. (2008). "Lipid droplets: a classic organelle with new outfits. Histochem." *Cell Biol.* **130**: 263-279.

Goizet C. et al. (2009). "Complicated forms of autosomal dominant hereditary spastic paraplegia are frequent in SPG10." *Hum Mutat.* **30**: E376-385.

Goodman J.M. (2008). "The gregarious lipid droplet." *J. Biol Chem.* **283**: 28005-28009.

Guo Y. et al. (2008). "Functional genomic screen reveals genes involved in lipid-droplet formation and utilization." *Nature* **453**: 657-661.

Hanada K. et al., (2007) "CERT and intracellular trafficking of ceramide." *Biochim Biophys Acta.* **1771**: 644-653.

Hansen J.J. et al. (2002). "Hereditary spastic paraplegia SPG13 is associated with a mutation in the gene encoding the mitochondrial chaperonin Hsp60." *Am J Hum Genet.* **70**(5): 1328-1332.

Harding A.E. (1993). "Hereditary spastic paraplegias."*Semin Neurol* **13**(4): 333-336.

Hetzer M. et al. (2001). "Distinct AAA-ATPase p97 complexes function in discrete steps of nuclear assembly." *Nat Cell Biol.* **3**: 1086–1091.

Hicke L. and **Schekman** R. (1989). "Yeast Sec23p acts in the cytoplasm to promote protein transport from the endoplasmic reticulum to the Golgi complex in vivo and in vitro." *EMBO J.* **8**(6): 1677-1684.

Kenwrick S. et al. (2000). "Neural cell recognition molecule L1: relating biological complexity to human disease mutations." *Hum Mol Genet.* **9**(6): 879-886.

Krogh et al. (2001) "Predicting transmembrane protein topology with a hidden Markov model: application to complete genomes." *J Mol Biol*. **305**: 567-580.

Kuerschner L. et al. (2008). "Imaging of lipid biosynthesis: how a neutral lipid enters lipid droplets." *Traffic.* **9**: 338-352.

Kumar Y. et al. (2006). "The obligate intracellular pathogen chlamydia trachomatis targets host lipid droplets." *Curr Biol.* **16**: 1646-1651.

Lardizabal K.D. et al. (2001). "DGAT2 is a new diacylglycerol acyltransferase gene family. Purification, cloning, and expression in insect cells of two polypeptides from *Mortierella ramanniana* with diacylglycerol acyltransferase activity." *J Biol Chem*. **276**: 38862-38869.

Latterich M. et al. (1995). "Membrane fusion and the cell cycle; Cdc48p participates in the fusion of ER membranes." *Cell.* **82**: 885-893.

Lee C. et al. (1989). "Construction of the endoplasmic reticulum." *J Cell Biol.* **109**: 2045-2055.

Levine T. and **Loewen** C. (2006). "Inter-organelle membrane contact sites: through a glass, darkly." *Curr Opin Cell Biol*. **18**: 371-378.

Liu P et al. (2003). "Chinese hamster ovary K2 cell lipid droplets appear to be metabolic organelles involved in membrane traffic." *J Biol Chem.* 2004; 279(5): 3787-3792. Epub **2003** Nov 3.

Liu P. et al. (2004). "Chinese hamster ovary K2 cell lipid droplets appear to be metabolic organelles involved in membrane traffic." *J Bio. Chem* **279**: 3787-3792.

Liu P. et al. (2008). "Rab-regulated membrane traffic between adiposomes and multiple endomembrane systems." *Methods Enzymol*. **439**: 327-337.

Mannan A.U. et al. (2006). "Spastin, the most commonly mutated protein in hereditary spastic paraplegia interacts with reticulon 1 an endoplasmic reticulum protein." *Neurogenetics*. **7**(2): 93-103.

Marcinkiewicz A. et al. (2006). "The phosphorylation of serine 492 of perilipin a directs lipid droplet fragmentation and dispersion." *J Biol Chem*. **281**: 11901-11909.

Martin S. and **Parton** R.G. (2006). "Lipid droplets: a unified view of a dynamic organelle." *Nat Rev Mol Cell Biol*. **7**: 373-378.

Masuda Y. et al. (2006). "Adrp/adipophilin is degraded through the proteasome-dependent pathway during regression of lipid-storing cells". *J Lipid Res*. **47**: 87-98.

McDermott C. et al. (2000). "Hereditary spastic paraparesis: a review of new developments." *J Neurol Neurosurg Psychiatry* **69**(2): 150-160.

McGookey D.J. and **Anderson** R.G. (1983). "Morphological characterization of the cholesteryl ester cycle in cultured mouse macrophage foam cells." *J Cell Biol.* **97**: 1156-1168.

Miyanari Y. et al. (2007). "The lipid droplet is an important organelle for hepatitis C virus production." *Nat Cell Biol.* **9**: 1089-1097.

Murphy R.C. et al. (2001) "Analysis of nonvolatile lipids by mass spectrometry." *Chem Rev.* **101**(2): 479-526.

Murphy S. et al. (2008). "Lipid droplet-organelle interactions; sharing the fats." *Biochim Biophys Acta* 1791(6): 441-447

Ohsaki Y. et al. (2006). "Cytoplasmic lipid droplets are sites of convergence of proteasomal and autophagic degradation of apolipoprotein B." *Mol Biol Cell* **17**: 2674-2683.

Olofsson S.O. et al. (2008). "Triglyceride containing lipid droplets and lipid droplet-associated proteins." *Curr Opin Lipidol.* **19:** 441-447.

Ostermeyer A, et al. (2001). "Accumulation of caveolin in the endoplasmic reticulum redirects the protein to lipid storage droplets." *J Cell Biol.* **152**: 1071-1078.

Ploegh H. (2007). "A lipid-based model for the creation of an escape hatch from the endoplasmic reticulum." *Nature* **448**: 435-438.

Prinz W.A. et al. (2000). "Mutants affecting the structure of the cortical endoplasmic reticulum in *Saccharomyces cerevisiae*." *J. Cell Biol.* **150**: 461-474.

Reid E. (1997). "Pure hereditary spastic paraplegia." *J Med Genet* **34**(6): 499-503.

Reid E. et al. (2002). "A kinesin heavy chain (KIF5A) mutation in hereditary spastic paraplegia (SPG10)." *Am J Hum Genet.* **71**(5): 1189-1194.

Robenek H. and **Severs** N.J. (2009). "Lipid droplet growth by fusion: insights from freeze-fracture imaging." *J Cell Mol Med.* **13**(11-12): 4657-4661.

Robenek H. et al. (2006). "Adipophilin-enriched domains in the ER membrane are sites of lipid droplet biogenesis". *J Cell Sci.* **119**: 4215–4224.

Robenek M.J. et al. (2004). "Lipids partition caveolin-1 from ER membranes into lipid droplets: updating the model of lipid droplet biogenesis." *Faseb J* **18**: 866-868.

Robenek H. et al. (2005). "PAT family proteins pervade lipid droplet cores." *J Lipid Res.* **46**: 1331-1338.

Rost B. and **Sander** C. (1993). "Secondary structure prediction of all-helical proteins in two states." *Protein Eng.* **6**(8): 831-836.

Rost B. *(*1996*). "*Topology prediction for helical transmembrane proteins at 86% accuracy." *Protein Sci.* **7***:* 1704–1718.

Rost B. et al. (1995). *"*Prediction of helical transmembrane segments at 95% accuracy." *Protein Sci.* **4**:521-533.

Roy L. et al. (2000). "Role of p97 and Syntaxin 5 in the assembly of transitional endoplasmic reticulum." *Mol. Cell. Biol.* **11**: 2529-2542.

Saito H. et al. (2004). "RTP family members induce functional expression of mammalian odorant receptors." *Cell.*;**119**(5):679-9.

Sanderson C.M. et al. (2006). "Spastin and atlastin, two proteins mutated in autosomal-dominant hereditary spastic paraplegia, are binding partners." *Hum Mol Genet* **15**(2): 307-318.

Schaffer J.E. and **Lodish** H.F. (1994). "Expression cloning and characterization of a novel adipocyte long chain fatty acid transport protein." *Cell* **79**: 427-436.

Schule R. et al. (2008). "SPG10 is a rare cause of spastic paraplegia in European families". *J. Neurol. Neurosurg. Psychiatry* **79**: 584-587.

Schulz T. and **Prinz** W. (2007) "Sterol transport in yeast and the oxysterol binding protein homologue (OSH) family." *Biochim Biophys Acta*. **1771**: 769-780.

Schwarz G.A. and **Liu** C.N. (1956). "Hereditary (familial) spastic paraplegia; further clinical and pathologic observations." *AMA Arch Neurol Psychiatry.* **75**(2): 144-162.

Seong et al. (2010). "Hereditary spastic paraplegia proteins REEP1, spastin, and atlastin-1 coordinate microtubule interactions with the tubular ER network." *J Clin Invest.* **120**(4): 1097-1110.

Shybata Y, et al. (2008). "The reticulon and DP1/Yop1p proteins form immobile oligomers in the tubular endoplasmic reticulum." *J Biol Chem.*; **283**(27): 18892-18904.

Soderblom C. and **Blackstone** C. (2006). "Traffic accidents: molecular genetic insights into the pathogenesis of the hereditary spastic paraplegias." *Pharmacol Ther.* **109**(1-2): 42-56.

Stobart A. K. et al. (1986). "Safflower microsomes catalyse oil accumulation in vitro: a model system". *Planta* **169**: 33-37.

Stone S.J. et al*. (2006). "Membrane topology and identification of key functional amino acid residues of murine acyl-CoA:diacylglycerol acyltransferase-2." J Biol Chem. **281***: 40273-40282*.

Stone S.S. et al. (2009). "The endoplasmic reticulum enzyme, DGAT2, is found in mitochondria-associated membranes and has a mitochondrial targeting signal that promotes its association with mitochondria." *J Biol Chem.* **284**: 5352-5361.

Sztalryd C. et al. (2006). "Functional compensation for adipose differentiation-related protein (ADFP) by Tip47 in an ADFP null embryonic cell line." *J Biol Chem.* **281**: 34341-34348.

Szymanski K. et al. (2007). "The lipodystrophy protein seipin is found at endoplasmic reticulum lipid droplet junctions and is important for droplet morphology." *Proc Natl Acad Sci*. USA **104**: 20890-20895.

Tauchi-Sato K. et al. (2002). "The surface of lipid droplets is a phospholipid monolayer with a unique fatty acid composition." *J Biol Chem*. **277**: 44507-44512.

Terasaki M. and **Jaffe** L.A. (1991). "Organization of the sea urchin egg endoplasmic reticulum and its reorganization at fertilization." *J Cell Biol*. **114**: 929-940.

Terasaki M. et al. (1986). "Microtubules and the endoplasmic reticulum are highly interdependent structures." *J Cell Biol*. **103**: 1557-1568.

Tobias et al. (2008). "The life of lipid droplets." *Biochim Biophys Acta*. **1791**(6): 459-466

Turrò S. et al. (2006). "Identification and characterization of associated with lipid droplet protein 1: A novel membrane-associated protein that resides on hepatic lipid droplets." *Traffic*.**7**(9): 1254-69.

Umlauf E. et al. (2004) *"*Association of stomatin with lipid bodies." *J Biol Chem* **279**: 23699–23709.

Vedrenne C. and **Hauri** H.P. (2006). "Morphogenesis of the endoplasmic reticulum: beyond active membrane expansion." *Traffic*, **7**: 639-646.

Voeltz G. et al. (2006). "A class of membrane proteins shap-ing the tubular endoplasmic reticulum." *Cell*. **124**(3): 573-586

Voeltz G.K. et al. (2006). "A class of membrane proteins shaping the tubular endoplasmic reticulum." *Cell*. **124**: 573-586.

Walther T.C. and **Farese** R.V.Jr. (2008). "The life of lipid droplets." *Biochim. Biophys. Acta* [Epub ahead of print] doi:10.1016/j.bbalip.2008.10.009.

Wang C. et al. (1999). "Hybrid hydrogels assembled from synthetic polymers and coiled-coil protein domains." *Nature*. **4**: 397(6718): 417-420.

Waterman-Storer C.M. and **Salmon** E.D. (1998). "Endoplasmic reticulum membrane tubules are distributed by microtubules in living cells using three distinct mechanisms." *Curr Biol*. **8**: 798-806.

Welte M.A. (2007). "Proteins under new management: lipid droplets deliver." *Trends Cell Biol*. **17**: 363-369.

Xu G. et al. (2005). "Post-translational regulation of Adrp by the ubiquitin/proteosome pathway." *J Biol Chem*. **280**: 42841-42847.

Xu G. (2006). "Degradation of perilipin is mediated through ubiquitination-proteasome pathway." *Biochim Biophys Acta* **1761**: 83-90.

Yabe I. et al. (2002). "Spastin gene mutation in Japanese with hereditary spastic paraplegia." *J Med Genet*. **39**(8): e46.

Zechner R. et al. (2005). "Lipolysis: pathway under construction." *Curr Opin Lipidol*. **16**: 333-340.

Zehmer J.K. et al. (2009). "A role for lipid droplets in inter-membrane lipid traffic." *Proteomics*. **9** (4): 914-921.

Zehmer J.K. et al. (2008). "Identification of a novel N-terminal hydrophobic sequence that targets proteins to lipid droplets." *J Cell Sci*. **121**: 1852-1860.

Züchner S. et al. (2006). "A new locus for dominant hereditary spastic paraplegia maps to chromosome 2p12." *Neurogenetics*. **7**(2): 127-129.